nature communications

Article

https://doi.org/10.1038/s41467-024-54074-8

Staphylococcal superantigens evoke temporary and reversible T cell anergy, but fail to block the development of a bacterium specific cellular immune response

Received: 18 March 2024

Accepted: 1 November 2024

Published online: 14 November 2024

Check for updates

Heran Zhang[1,3], Ian R. Monk[1,3], Jessica Braverman[1], Claerwen M. Jones[2], Andrew G. Brooks[1], Timothy P. Stinear[1] & Linda M. Wakim[1]

Superantigens (sAgs) are bacterial virulence factors that induce a state of immune hyperactivation by forming a bridge between certain subsets of T cell receptor (TCR) β chains on T lymphocytes, and class II major histocompatibility complex (MHC-II) molecules; this cross-linking leads to indiscriminate T cell activation, cytokine storm and toxic shock. Here we show that sAg exposure drives the preferential expansion of naive and central memory T cell subsets, but not effector or resident memory T cells, which instead, hyper release pro-inflammatory cytokines. A targeted therapeutic approach to minimise cytokine release by effector memory T cells attenuated sAg-induced cytokine release. Irrespective of antigen experience, sAg activation does not render mature T cells permanently dysfunctional, and full restoration of effector function is observed following a transient and reversible anergy. Moreover, we show that in the face of sAg induced immune hyperactivation, an intact bacterium-specific $CD4^+$ T cell response can be mounted.

Superantigens (sAgs) are the most potent T cell mitogens ever discovered. These bacterial virulence factors comprise of a large family of very stable, secreted exotoxins that are produced primarily by *Staphylococcus aureus* and group A *Streptococci*[1]. sAgs mediate their pathological effects by crosslinking subsets of T-cell receptor (TCR) β chains and costimulatory molecules (CD28) on T lymphocytes, and class II major histocompatibility complex (MHC-II) molecules on antigen-presenting cells. This bridge forms outside of the conventional peptide-binding groove and leads to aberrant and widespread activation of T cells[2–5]. Compared to a conventional antigen-induced T-cell response where 0.0001–0.001% of the body's T-cells are activated[6], sAgs can activate up to 20% of all T cells[7]. This can lead to toxic shock syndrome (TSS)[8] due to a massive production of proinflammatory cytokines, such as interferon-gamma (IFNγ) and tumour necrosis factor alpha (TNFα)[9]. While the capacity of sAgs to induce non-specific T cell proliferation and hypercytokinemia is well-established, there is inconsistency as to whether this stimulation incapacitates and deletes T cells, or whether T cells retain normal functionality post sAg exposure.

Why bacteria express such potent T cell mitogens remains unclear, although the ubiquity of sAgs in *S. aureus* clinical isolates implies that these toxins are likely contributing to the evolutionary fitness of these bacteria. At first glance, it seems counterintuitive for bacteria to intentionally trigger a robust pro-inflammatory state, as inflammation promotes the resolution of many bacterial infections. However, this ability is assumed to be an immune subversion tactic. Bacteria secreted sAgs are proposed to obstruct the development of a pathogen specific cellular immune response by blocking bacteria specific T cell activation and memory T cell development, although direct evidence of this interference is

[1]Department of Microbiology and Immunology, The University of Melbourne, at the Peter Doherty Institute for Infection and Immunity, Melbourne, VIC 3000, Australia. [2]Biomedicine Discovery Institute and Department of Biochemistry and Molecular Biology, Monash University, Melbourne, VIC 3800, Australia. [3]These authors contributed equally: Heran Zhang, Ian R. Monk. e-mail: wakiml@unimelb.edu.au

lacking, primarily because there are limited tools available to track bacteria-reactive T cells.

In the current study, we set out to determine the fate and functionality of naïve and memory (central, effector and resident) T cell subsets following sAg exposure and explore whether sAg expressing bacteria thwart the development of a pathogen specific memory CD4$^+$ T cell response. To do this we utilized murine T cells with fixed TCR, transgenic mice expressing the human leukocyte antigen (HLA)-DR4 which are sensitive to sAg activity, and a panel of *S. aureus* strains engineered to express sAgs and trackable CD4$^+$ T cell epitopes. Using these tools, we show that the fate and responsiveness of T cells following sAg exposure is influenced by the maturity and location of the T cell population. Moreover, we show that a fully functional bacterium-specific CD4$^+$ T cell response can be initiated in the face of sAg induced immune hyperactivation.

Results

Differential activation and expansion of human CD4$^+$ T cell subsets following exposure to bacteria derived sAgs

We prepared a panel of sAg-expressing or -deficient strains of *S. aureus*, consisting of the sAg deficienct *S. aureus* strain JKD6159[10], that we engineered to express the sAg Staphylococcal enterotoxin A (SEA) (JKD6159::*sea*) or Staphylococcal enterotoxin B (SEB) (JKD6159::*seb*); *S. aureus* strain Newman, that endogenously expresses the SEA sAg; and *S. aureus* strain COL, that produces the sAgs SEB, SEQ and SEK. As controls, we also generated Newman and COL sAg-null mutants (Newman△*sea*, COL△*seb*△*sek*△*seq*). We first confirmed that these bacterial derived sAgs were produced at sufficient quantities to trigger bulk CD4$^+$ T cell activation, expansion and cytokine production. To do this, unfractionated peripheral blood mononuclear cells (PBMCs) were left untreated or stimulated with bacteria supernatants (1%v/v) harvested from overnight cultures of JKD6159, JKD6159::*sea*, JKD6159::*seb*, Newman, and Newman△*sea* and 48 h later the percentages of CD4$^+$ T cells expressing the activation marker CD69$^+$ was measured by flow cytometry. We observed 4–11% of total CD4$^+$ T cells rapidly induced CD69$^+$ expression when cultured with supernatants collected from sAgs$^+$ strains (JKD6159::*sea*, JKD6159::*seb*, Newman) while, importantly, exposure to supernatants derived from sAg deficient or null mutant strains (JKD6159, Newman△*sea*) failed to evoke CD4$^+$ T cell activation (Fig. 1a, b). We next tested whether this assay could be used to assess polyclonal T cell expansion and cytokine release. Unfractionated carboxyfluorescein succinimidyl ester (CFSE) labelled PBMCs were cultured with autologous monocyte derived DCs (moDCS) for 7 days either alone, or in presence of titrated doses of bacterial supernatants from JKD6159, JKD6159::*sea*, JKD6159::*seb*, Newman, and Newman△*sea* strains. The expansion of total CD4$^+$ T cells, as assessed by a loss of CFSE dye, and the production of pro-inflammatory cytokines IFNγ and TNFα was measured following a brief in vitro restimulation. When PBMCs were stimulated with supernatants derived from sAg deficient or null mutant strains (JKD6159, Newman△*sea*) no CD4$^+$ T cell proliferation and background levels of IFNγ and TNFα production were observed (Fig. 1c–h). Conversely, exposure to 0.1% or 1.0% (v/v) of bacterial supernatant derived from strains JKD6159::*sea* or JKD6159::*seb*, that were engineered to express SEA and SEB respectively, or strain Newman, which endogenously carries the SEA sAg, triggered significant CD4$^+$ T cell proliferation and cytokine production when compared to unstimulated controls (Fig. 1c–h). Exposure to higher concentrations (10% v/v) of bacterial supernatant from sAg$^+$ strains did not induce CD4$^+$ T cell proliferation or cytokine production, as this dose significantly reduced cell viability (Fig S1a).

We next determined whether sAgs differentially activated human CD4$^+$ T cell subsets. To this end, CFSE labelled, sort-purified, naïve CD4$^+$ T cells (Tn; CD27$^+$CD45RA$^+$), effector memory CD4$^+$ T cells (Tem; CD27$^-$CD45RA$^-$) and central memory CD4$^+$ T cells (Tcm; CD27$^+$CD45RA$^-$) were cultured with autologous HLA-DR$^+$ cells for 7 days (Fig. 1i) with or without 0.1% (v/v) of bacterial supernatant from sAg$^+$ (Newman, COL, JKD6159::*sea* and JKD6159::*seb*) or sAg deficient strains (Newman△*sea*, Col△*seb*△*seq*△*sek*, JKD6159) and CD4$^+$ T cell expansion and cytokine production, following a brief in vitro restimulation was measured. Both Tn and Tcm CD4$^+$ T cell subsets underwent significantly greater (6-20 fold) expansion than Tem when cultured with bacterial supernatant derived from sAg$^+$ strains (Newman, COL, JKD6159::*sea* and JKD6159::*seb*) (Fig. 1j). When measuring cytokine production, the opposite hierarchy was observed, with CD4$^+$ Tem producing significantly more TNFα than Tn and Tcm subsets following stimulation with sAg$^+$ strains (Newman, COL, JKD6159::*sea* and JKD6159::*seb*) (Fig. 1k). Again, when cultured with supernatant derived from sAg$^-$ strains (Newman△*sea*, Col△*seb*△*seq*△*sek*, JKD6159) no CD4$^+$ T cell subset divided or produced cytokines (Fig. 1j, k). These data suggest that sAg exposure causes robust proliferation of both CD4$^+$ Tn and Tcm subsets, but not Tem, which instead, hyper-release pro-inflammatory cytokines.

Differential activation and expansion of mouse CD4$^+$ T cell subsets following exposure to bacterial-derived sAgs

sAgs have an activation bias, preferentially stimulating T cells expressing specific TCR Vβ chains[7]. Thus, TCR repertoire diversity across subsets of human CD4$^+$ T cells may influence the sAg triggered activation profile observed above. To eliminate this variable, we next established a mouse model that tested the fate and functionality of sAg stimulated T cell subsets generated from TCR transgenic mice that express a fixed, monoclonal TCR. As the binding affinity of sAgs to murine MHC-II is low, antigen presenting cells used in these experiments were derived from human leukocyte antigen (HLA) transgenic mice (hereafter referred to as DR4-DQ8 mice) which have been engineered to express the human HLA-DR4-DQ8 molecule[11]. Others have shown the DR4-DQ8 mice are sensitive to sAg activity[12,13]. To confirm this, titrated doses of bacterial supernatants from JKD6159, JKD6159::*sea*, JKD6159::*seb*, Newman, and Newman△*sea* strain were added to cultures of CFSE labelled purified polyclonal CD4$^+$ T cells isolated from C57BL/6 mice and splenic dendritic cells (DCs) enriched from either C57BL/6 or DR4-DQ8 mice. CD4$^+$ T cell expansion, as assessed by a loss of CFSE dye, was measured 4 days later. It is noteworthy, that the assessment of the activation status of the DCs in cultures revealed that the concentrations of bacterial supernatant used in this assay failed to trigger significant DC activation (Fig S1b). As expected, the supernatants derived from cultures of sAg$^-$ bacteria (Newman△*sea* and JKD6159) did not drive CD4$^+$ T cell proliferation irrespective of the origin of the antigen presenting cells (Fig. 2a). In contrast, sAg$^+$ supernatant evoked robust CD4$^+$ T cell expansion although this was limited to conditions that contained human HLA expressing DR4-DQ8 DCs, with negligible levels of CD4$^+$ T cell expansion being detected in the presence of murine MHC-II expressing C57BL/6 DCs (Fig. 2a). The SEA and SEB sAgs preferentially activate Vβ11 and Vβ8 murine T cells, respectively, and the assessment of the proportion of CD4$^+$ T cells in these cultures expressing these Vβ TCRs confirmed this predicated preferential TCR skewing (Fig. 2b, c).

We next assayed the activation profile following sAg exposure of CD4$^+$ and CD8$^+$ T cell subsets isolated from TCR transgenic mouse strains that express a monoclonal TCR to standardise the TCR repertoire across all T cell subsets. The SMARTA.Thy1.1 CD4 TCR transgenic mice (Vα2.3/Vβ8.3), which are reactive against the LCMV $GP_{61\text{-}80}$ epitope were selected as they express Vβ8.3 restricted CD4$^+$ T cells, and therefore are expected to react to sAg SEB, while F5.CD45.1 CD8 TCR transgenic mice, which are responsive to the $NP_{366\text{-}374}$ epitope of influenza virus (Vα4/Vβ11), were selected as they express CD8$^+$ T cells that are Vβ11 restricted, and should respond to sAg SEA. Naïve SMARTA CD4$^+$ T cells (CD90.1$^+$CD4$^+$CD44$^-$) and SMARTA Tem (CD90.1$^+$CD4$^+$CD44$^+$CD62L$^-$) and Tcm (CD90.1$^+$CD4$^+$CD44$^+$CD62L$^+$) CD4$^+$ T cells (Fig. 2d), which we purified from memory mice

https://doi.org/10.1038/s41467-024-54074-8

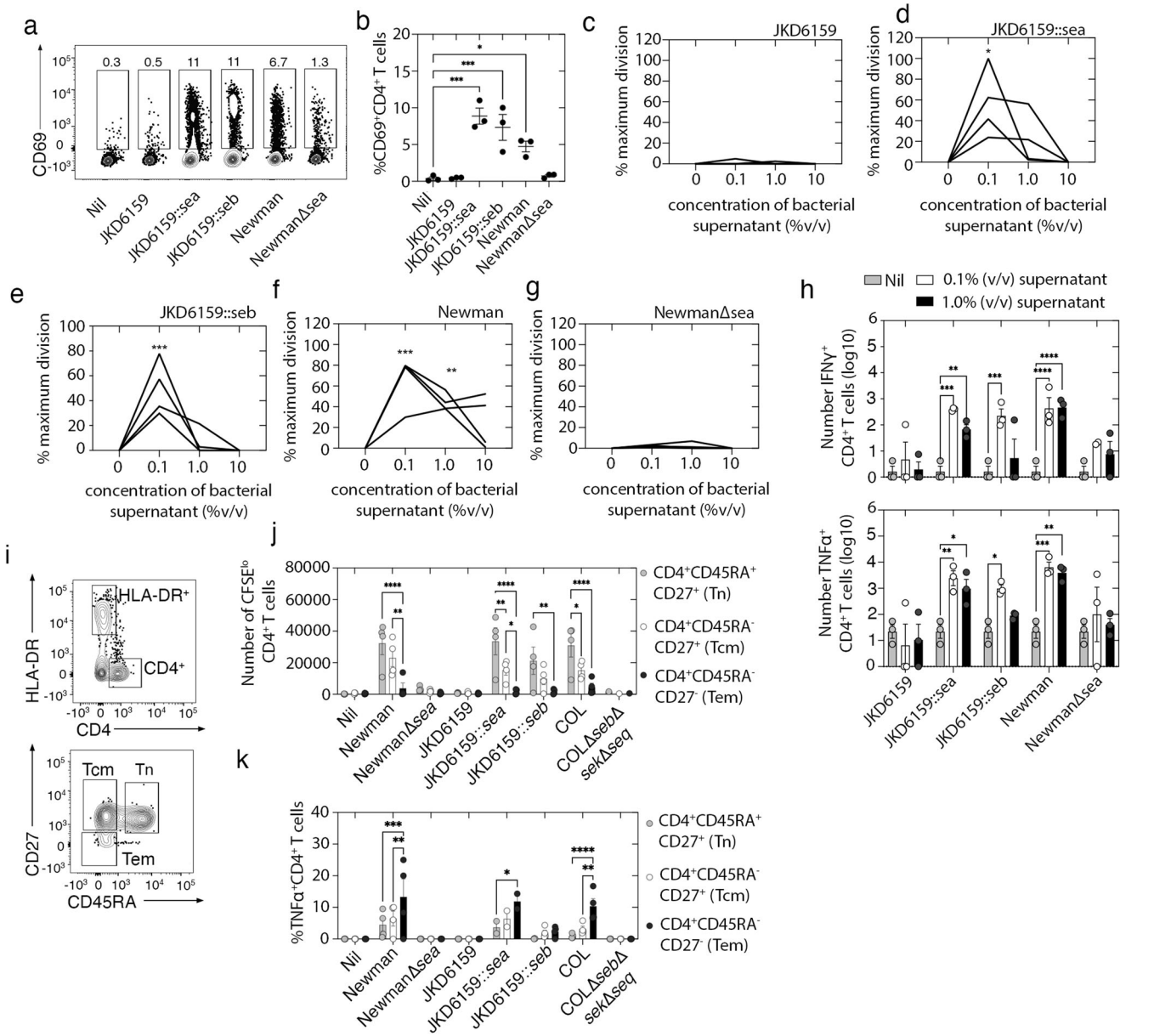

Fig. 1 | The differential activation and expansion of human CD4⁺ T cell subsets following exposure to bacteria derived sAgs. 250,000 PBMCs were cultured for 48 h either alone (Nil) or with 1% v/v of bacterial supernatants harvested from overnight cultures of the following strains, JKD6159, JKD6159::*sea*, JKD6159::*seb*, Newman, Newman△*sea* and the percentages of CD4⁺ T cells expressing the activation marker CD69 was measured by flow cytometry. **a** Representative FACs profiles gated on CD4⁺ T cells showing the percentage of CD69⁺ cells. **b** The percentage of CD69⁺CD4⁺ T cells. Symbols represent individual donors, bars represent the mean ± SEM. Data pooled from 3 donors (one way ANOVA, Dunnett's multiple comparison). **c**–**g** 20,000 moDCs were cultured (1:1) with matched CFSE labelled bulk PBMCs for 7 days either alone (Nil) or with 0.1%, 1.0% or 10% v/v of bacterial supernatants harvested from overnight cultures of the following strains, JKD6159, JKD6159::*sea*, JKD6159::*seb*, Newman, Newman△*sea*. The absolute number of divided (CFSE^{lo}) CD4⁺ T cells was measured by flow cytometry. Graphs depict the percentages of maximum CD4⁺ T cell division per experiment (lines represent individual donors, Two-way ANOVA, Dunnett's multiple comparison). **h** The absolute number of IFNγ and TNFα producing CD4⁺ T cells, measured by intracellular cytokine staining, following a brief in vitro restimulation with bacterial supernatant. Symbols represent individual donors, bars represent the mean ± SEM. Data pooled from 3 donors (log transformation, Two-way ANOVA, Dunnett's multiple comparison). **i** Representative flow cytometry profiles gated on HLA-DR⁺ cells and CD4⁺ T cells, which were further subdivided into naïve (CD27⁺CD45RA⁺), Tcm (CD27⁺CD45RA⁻) and Tem (CD27⁻CD45RA⁻). **j**–**k** 20,000 HLA-DR⁺ cells and CFSE labelled CD4⁺ Tcm, Tem and Tn subsets sort purified from matched donor PBMCs were cultured 1:1 for 7 days either alone, (Nil) or with 0.1% (v/v) of bacterial supernatants harvested from overnight cultures of the following strains, JKD6159, JKD6159::*sea*, JKD6159::*seb*, Newman, Newman△*sea*, COL or COL△*seb*△*sek*△*seq*. **j** The absolute number of divided (CFSE^{lo}) CD4⁺ T cells and (**k**) the proportion producing TNFα (TNFα⁺) following a brief in vitro restimulation. Symbols represent individual donors, bars represent the mean ± SEM. Data pooled from 4 donors (two way ANOVA, Tukey's multiple comparison). *$p < 0.5$, **$p < 0.01$, ***$p < 0.001$, and ****$p < 0.0001$.

(generated as described in material and methods) were CFSE labelled and cultured with splenic DCs enriched from DR4-DQ8 mice, either alone (Nil), or with bacterial supernatants from JKD6159, JKD6159::*seb*, COL and COL△*seb*△*seq*△*sek* strains and 4 days later, CD4⁺ T cell expansion, and cytokine production following a brief in vitro restimulation was measured. Tn and Tcm SMARTA CD4⁺ T cell subsets proliferated when cultured with bacteria supernatant derived from SEB sAg⁺ strains (COL, JKD6159::*seb*), while again Tem cells failed to expand (Fig. 2e). The reduced proliferation of Tem following SEB sAg exposure could not be attributed to activation induced cell

https://doi.org/10.1038/s41467-024-54074-8

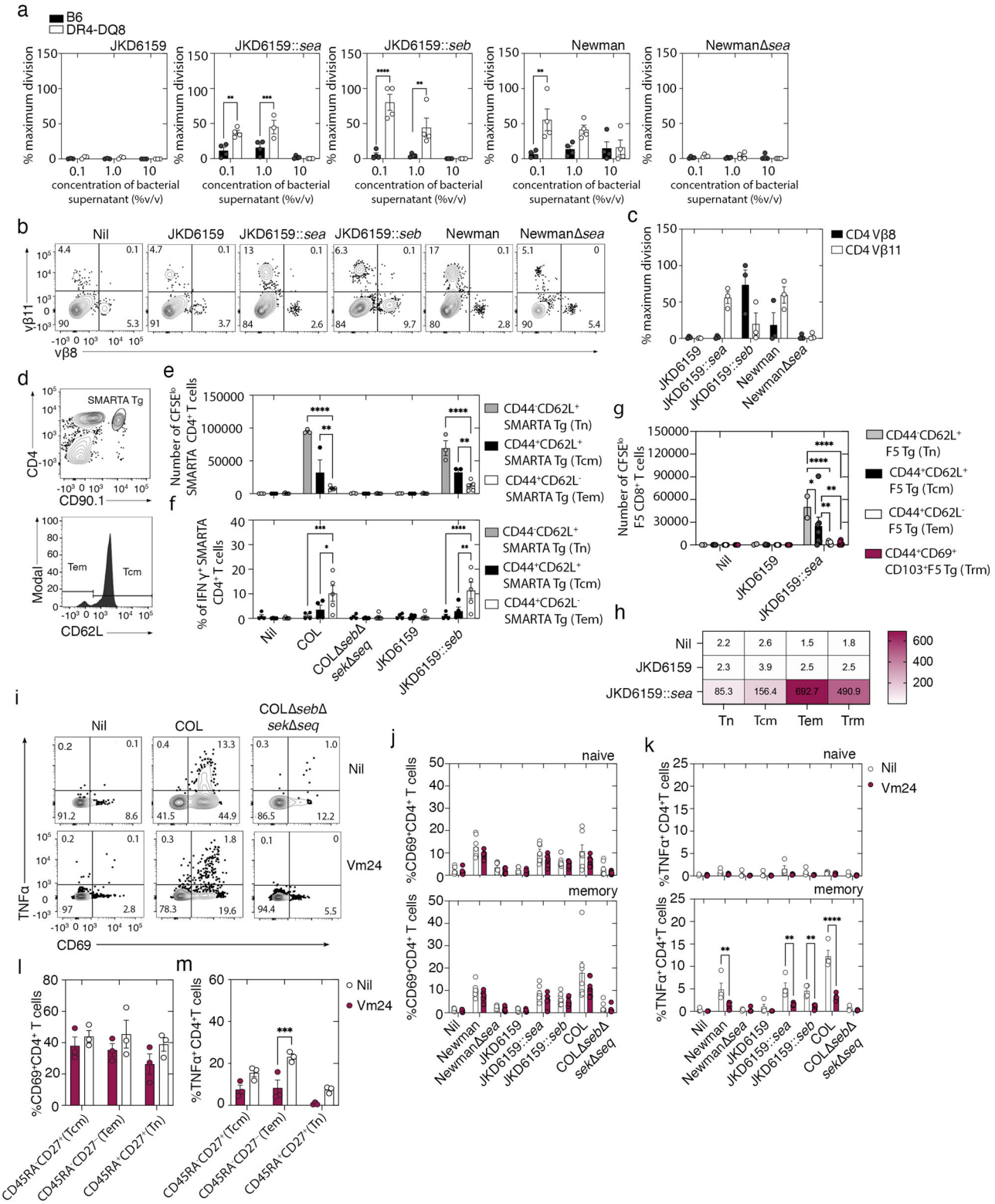

death, a cell death pathway Tem are highly sensitive to following strong TCR engagement, as assessment of the proportion of viable, apoptotic and dead cells in these cultures was comparable across the three T cells subsets (Fig S2a). Exposure to bacteria supernatant derived from SEB sAg$^+$ strains resulted in significant IFNγ production by Tem CD4$^+$ T cells when compared to the amount generated by either Tn or Tcm (Fig. 2f), a phenotype that was further confirmed when the concentrations of a panel of pro-inflammatory cytokines were measured in culture supernatants (Fig S2b). Interestingly, in addition to IFNγ, we also detected elevated levels of IL-17 in the culture supernatants of SEB sAg exposed Tem CD4$^+$ T cells. This result is consistent with previous reports that show Tem, but not Tn, produce high levels of IL-17 post sAg exposure[14–16]. Again, supernatants derived from sAg$^-$ strains failed to activate any of the SMARTA CD4$^+$ T cell subsets (Fig. 2e, f). When we repeated this experiment but instead used Vβ11 restricted naïve F5 CD8$^+$ T cells (CD45.1$^+$CD8$^+$CD44$^-$) and F5 Tem (CD45.1$^+$CD8$^+$CD44$^+$CD62L$^-$) and Tcm (CD45.1$^+$CD8$^+$CD44$^+$CD62L$^+$) CD8$^+$ T cells, which we purified

Fig. 2 | Exposure to bacteria derived sAgs preferentially drives cytokine release by memory CD4⁺ T cells. 50,000 DCs purified from the spleen of B6 and DR4-DQ8 mice were cultured 1:1 with CFSE labelled CD4⁺ T cells enriched from B6 mice for 4 days either alone (Nil), or with 0.1%, 1%, or 10% (v/v) supernatants harvested from overnight cultures of JKD6159, JKD6159::*sea*, JKD6159::*seb*, Newman, and Newman△*sea*. The absolute number of divided (CFSE^{lo}) CD4⁺ T cells was measured by flow cytometry. **a** The graphs depict percentages of maximum CD4⁺ T cell division. Bars represent the mean ± SEM. Data pooled from 4 independent experiments (Two-way ANOVA, Sidak's multiple comparison). **b** Representative flow cytometry profiles gated on total CD4⁺ T cells (0.1% v/v condition) depicting Vβ8 and Vβ11 expression. **c** The graphs depict percentages of maximum Vβ8⁺CD4⁺ T and Vβ11⁺CD4⁺ T cell division. Bars represent the mean ± SEM. Data pooled from 3 independent experiments. **d** Mice seeded with high numbers of in vitro activated SMARTA.CD90.1⁺ CD4⁺ T cells and rested for 10 days to generate memory mice. Representative flow cytometry profiles depicting the proportion of Tem (CD62L⁻) and Tcm (CD62L⁺) cells. **e**, **f** 50,000 splenic DCs purified from DR4-DQ8 mice were cultured 2:1 with CFSE labelled CD4⁺ naïve SMARTA.CD90.1⁺ (Tn) T cells or SMARTA Tcm (CD62L⁺) or Tem (CD62L⁻) CD4⁺ T cells subsets purified from memory mice (generated as described in material and methods) for 4 days either alone (Nil), or with 0.1% v/v supernatants harvested from overnight cultures of COL, COL△*seb*△*sek*△*seq* COL, JKD6159 or JKD6159::*seb* (**e**). The absolute number of divided cells (CFSE^{lo}) CD4⁺ SMARTA.CD90.1⁺ T cells was measured by flow cytometry. Bars represent the mean ± SEM. Data pooled from 5 independent experiments (Two-way ANOVA, Sidak's multiple comparison). **f** The proportion of IFNγ producing Tn, Tcm and Tem SMARTA CD4⁺ T cells, measured by intracellular cytokine staining following a brief in vitro restimulation with bacterial supernatant, was measured by flow cytometry. Graph depicts the percentage of SMARTA CD4⁺ T cells synthesizing IFNγ. Bars represent the mean ± SEM. Data pooled from 5 independent experiments (two-way ANOVA, Tukey's multiple comparison). **g**, **h** 50,00 splenic DCs purified from DR4-DQ8 mice were cultured 2:1 with CFSE labelled CD8⁺ F5.CD45.1⁺ Tcm (CD62L⁺), Tem (CD62L⁻) or lung Trm (CD103⁺CD69⁺) CD8⁺ T cells subsets purified from memory mice (generated as described in material and methods) for 4 days either alone (Nil), or with 0.1% v/v supernatants harvested from overnight cultures of JKD6159 or JKD6159::*sea*. **g** The absolute number of divided cells (CFSE^{lo}) CD8⁺ T cells was measured by flow cytometry. Bars represent the mean ± SEM. Data pooled from 7 experiments (two-way ANOVA, Tukey's multiple comparison). **h** Heatmap shows the average concentration of IFNγ in the supernatant measured by cytometric bead array. **i**–**k** 200,000 PBMCs were cultured for 24 h either alone (Nil) or with 0.1% v/v of bacterial supernatants harvested from overnight cultures of a panel of *S. aureus* strains, with or without 1 nM Vm24, and the percentages of CD4⁺ T cells expressing the activation marker CD69 and the proportion of naïve (CD45RA⁺) or memory (CD45RA⁻) CD4⁺ T cells expressing TNFα was measured by flow cytometry. **i** Representative FACs profiles gated on CD4⁺ T cells showing the percentage of CD69⁺ and TNFα⁺ cells (**j**). The percentage of CD69⁺CD4⁺ T cells and (**k**) percentage of TNFα⁺ CD4⁺ T cells. Symbols represent individual donors, bars represent the mean ± SEM. Data pooled from 6 donors (one way ANOVA, Dunnett's multiple comparison). **l**–**m** CD4⁺ Tcm, Tem and Tn subsets sort purified from donor PBMCs were cultured 1:1 with allogenic HLA-DR4⁺ cells for 24 h with 0.1% (v/v) of bacterial supernatants harvested from an overnight culture of the COL strain with or without 1 nM Vm24, and the percentages of CD4⁺ T cells (**l**) expressing the activation marker CD69 and (**m**) the proportion expressing TNFα was measured by flow cytometry. Symbols represent individual donors, bars represent the mean ± SEM. Data pooled from 3 donors (Two-way ANOVA, Sidak's multiple comparison) $^{*}p < 0.5$, $^{**}p < 0.01$, $^{***}p < 0.001$, and $^{****}p < 0.0001$.

from memory mice and stimulated with DR4-DQ8 DCs and SEA sAg⁺ bacterial supernatants, we again observed a very similar activation and cytokine profile across the profiled T cell subsets (Fig S2c-d). Moreover, when endogenous Tem and Tcm Vβ8⁺ influenza nucleoprotein (NP)-specific CD8⁺ T cells were purified from mice previously infected with influenza virus and stimulated with DR4-DQ8 DCs and SEB sAg⁺ bacterial supernatants, we once again observed that sAg exposure causes robust proliferation of CD8⁺ Tcm, but not Tem, which instead, hyper-released pro-inflammatory cytokines (Fig S2e-g).

We next tested how tissue-bound Trm cells responded following sAg exposure. To this end, we purified F5 Tem (CD45.1⁺CD8⁺CD44⁺CD62L⁻) and Tcm (CD45.1⁺CD8⁺CD44⁺CD62L⁺) CD8⁺ T cells from the spleen, and F5 Trm (CD45.1⁺CD8⁺CD44⁺CD103⁺CD69⁺) CD8⁺ T cells from the lung of mice seeded with naïve F5.CD45.1⁺ T cells and infected 20 days prior intranasally with X-31(DAM), an influenza virus strain we engineered to express the NP epitope recognised by F5 CD8⁺ T cells[17]. As described above, these memory T cell subsets, as well as naïve F5 CD8⁺ T cells, were CFSE labelled and stimulated with DR4-DQ8.F1 DCs and bacterial supernatants from either JKD6159 or JKD6159::*sea* or as a control, cognate peptide. Assessment of the total number of divided F5 CD8⁺ T cells showed that while all CD8⁺ T cell subsets proliferated following stimulation with cognate peptide (Fig S2h), Tn and Tcm, but not Tem or Trm expanded when cultured with bacterial supernatant derived from SEA sAg⁺ strains (JKD6159::*sea*) (Fig. 2g). Quantitation of the amount of IFNγ produced by these CD8⁺ T cell subsets revealed increased IFNγ release by Tem and Trm compared to Tcm and Tn (Fig. 2h). Collectively, these data show that sAg exposure drives the preferential expansion of CD4⁺ and CD8⁺ Tn and Tcm subsets, but not Tem and Trm, which instead, release pro-inflammatory cytokines. Thus, a refined targeted therapeutic approach to minimise cytokine production by Tem cells may serve to attenuate sAg-induced cytokine storm.

Voltage-gated $K_V1.3$ channel inhibitors which are being developed as a clinical treatment for autoimmune conditions[18,19] have been reported to preferentially target Tem cells[20–22], reducing their expansion and cytokine production. Because Kv1.3 channels are expressed at elevated concentrations on Tem cells alone (Fig S3), this therapy does not impair Tn or Tcm responses. We next set out to determine whether blocking Kv1.3 channels could limit sAg induced cytokine release. As the differential distribution of Kv1.3 channels between Tem, Tn and Tcm is restricted to human T cells, we cultured unfractionated PBMCs with bacteria supernatants (0.1% v/v) harvested from overnight cultures of JKD6159, JKD6159::*sea*, JKD6159::*seb*, Newman, Newman△*sea*, COL and COL△*seb*△*seq*△*sek* with or without 1 nM Vm24 toxin (Kv1.3 blocker) and 24 hrs later the percentages of CD4⁺ T cells expressing the activation marker CD69⁺ and the proportion of naïve (CD45RA⁺) and memory (CD45RA⁻) CD4⁺ T cells synthesizing TNFα was measured by flow cytometry. While both naïve and memory CD4⁺ T cells upregulated CD69 following exposure to sAg containing bacterial supernatants (Fig. 2I, j), consistent with earlier results, we observe the majority of cytokine producing cells to be antigen experienced cells, and importantly, the introduction of the Kv1.3 blocker could significantly attenuate sAg induced cytokine production by these cells (Fig. 2i–k). Moreover, when we repeated this experiment but instead sort purified Tem, Tcm and Tn cells prior to culture with bacterial supernatant and the Vm24 inhibitor, we observed preferential reduction of cytokine production by sAg exposed Tem cells (Fig. 2l, m).

Naïve and memory T cells remain functional following sAg activation

We next examined the fate of naïve and memory T cells following sAg activation, and tested whether these cells could mount a recall response. To do this, naïve F5 CD8⁺ T cells were activated in vitro with DR4-DQ8.F1 splenic DCs pulsed with either JKD6159::*sea* bacterial supernatant or $NP_{366\text{-}374}$ cognate peptide. Assessment of the phenotype of the F5 CD8⁺ T cells after 4 days of culture revealed a similar profile irrespective of whether the cells were activated by cognate peptide or SEA sAg with most cells upregulating CD44 and CD69 and downregulating CD62L (Fig. 3a). Next, we adoptively transferred 5×10^6 peptide- or sAg-activated F5 CD8⁺ T cells into naïve C56BL/6 mice which we rested for 10 days to allow for memory development[23]. Peptide and sAg activated F5 CD8⁺ memory T cells were detected at similar frequencies and equivalent ratios of Tcm:Tem in both the

https://doi.org/10.1038/s41467-024-54074-8

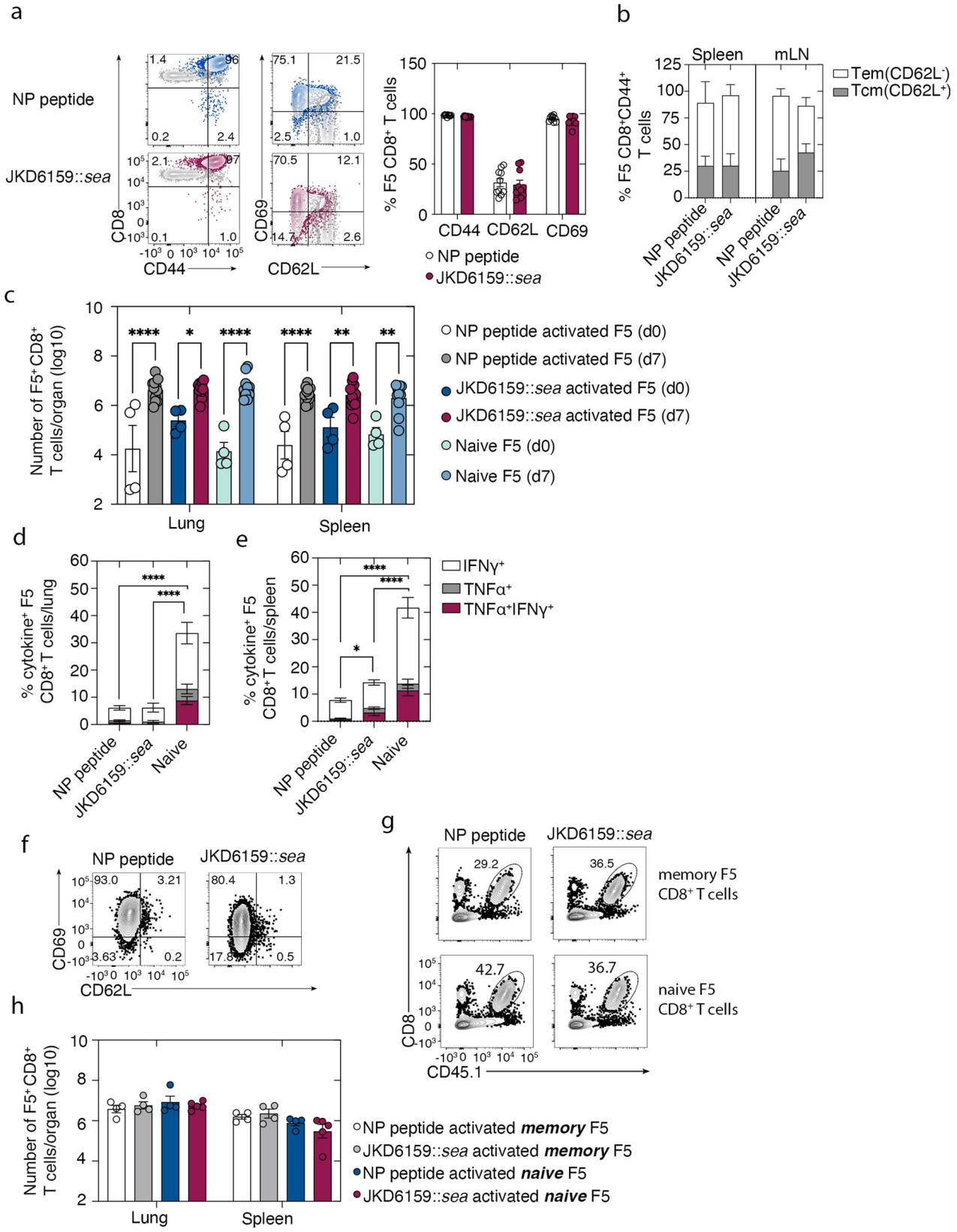

spleen and mediastinal LN (mLN) (Fig. 3b). To test the recall expansion of peptide and sAg activated F5 CD8$^+$ T cells, cohorts of mice generated as described above, in addition to a cohort that received 5×10^6 naïve F5 CD8$^+$ T cells were infected intranasally with X-31(DAM) and the size and functionality of F5 CD8$^+$ T cells were assessed 7 days post challenge. Naïve, peptide and sAg activated F5 CD8$^+$ T cells expanded to equivalent sized effector T cell populations in both the lung and spleen (Fig. 3c). Assessment of cytokine production following a brief in vitro stimulation revealed that F5 CD8$^+$ T cells in the lung, independent of the original activation method, synthesized equvalent levels of IFNγ and TNFα. Slightly improved cytokine production by sAg activated F5 CD8$^+$ T cells was detected in the spleen, albeit both in vitro

Fig. 3 | Naïve and memory T cells remain functional following sAg activation. **a** 5×10^6 naïve F5.CD45.1$^+$ CD8$^+$ T cells activated in vitro with either NP-peptide or 0.1% v/v JKD6159::*sea* bacteria supernatant were seeded into B6 mice and were left to rest for 10 days. Representative flow cytometry profiles showing the level of expression of CD44, CD69 and CD62L on the peptide and sAg activated F5.CD45.1$^+$ cells prior to transfer compared to unstimulated naïve cells (grey contours). Graph depicts the proportion of F5$^+$ CD8$^+$ T cells expressing CD44, CD69 and CD62L following peptide or sAg activation. Bars represent the mean ± SEM, and symbols represent individual cultures. Data pooled from 10 experimental cultures. **b** The proportion of Tem (CD62L$^-$) and Tcm (CD62L$^+$) F5.CD45.1$^+$ CD8$^+$ T cells in the spleen and mLN. Bars represent the mean ± SEM ($n = 2$ or 4 mice per group). **c** Mice generated as described in **a** or mice receiving 5×10^6 naïve F5.CD45.1$^+$ CD8$^+$ T cells were either left untreated (d0) or were infected intranasally with 10^4 PFU X31(DAM) and 7 days later the absolute number of F5.CD45.1$^+$ CD8$^+$ T cells in the spleen and lung were measured. Symbols represent individual mice, bars represent the mean ± SEM ($n = 4$–11 mice per group, Two-way ANOVA, Tukey's multiple comparison). The proportion of F5.CD45.1$^+$ T cells in the (**d**) lung and (**e**) spleen producing TNFα and/or IFNγ following a brief in vitro stimulation was measured by flow cytometry. Bars represent the mean ± SEM, and symbols represent individual mice ($n = 5$–11 mice cohort, Two-way ANOVA, Sidak's multiple comparison). **f**–**h** 5×10^6 naïve or memory F5.CD45.1$^+$ CD8$^+$ T cells activated in vitro with either NP-peptide or 0.1% v/v JKD6159::*sea* bacteria supernatant were seeded into B6 mice and were left to rest for 10 days were infected intranasally with 10^4 PFU X31(DAM) (**f**) Representative flow cytometry profiles showing the level of expression of CD69 and CD62L on the peptide and sAg activated memory F5.CD45.1$^+$ T cells prior to transfer. **g** Representative flow cytometry profiles of the lung on day 7 post infection (h) The absolute number of F5.CD45.1$^+$ CD8$^+$ T cells in the spleen and lung were measured on day 7 post infection. Symbols represent individual mice, bars represent the mean ± SEM ($n = 4$ or 5 mice per group, Two-way ANOVA, Tukey's multiple comparison). *$p < 0.5$, **$p < 0.01$, ***$p < 0.001$, and ****$p < 0.0001$.

activated cell populations synthesized lower amounts of cytokines compared to naïve F5 CD8$^+$T cells (Fig. 3d, e).

We next used a similar model to determine the fate and test the recall response of memory T cell following sAg activation. To this end, Tcm (CD45.1$^+$CD8$^+$CD44$^+$CD62L$^+$) F5 CD8$^+$ T cells, purified from memory mice, and as a control naïve F5 CD8$^+$ T cells, were stimulated in vitro with DR4-DQ8.F1 splenic DCs pulsed with either JKD6159::*sea* bacterial supernatant or $NP_{366\text{-}374}$ cognate peptide prior to injection into naïve B6 mice that we rested for 10 days, at which point we challenged these animals intranasally with X-31(DAM). Again, the phenotype of memory F5 CD8$^+$ T cells following peptide or SEA sAg activation matched, with most cells upregulating CD69 and downregulating CD62L (Fig. 3f). Assessment of the absolute number of F5 CD8$^+$ T cells in the spleen and lung on day 7 post influenza challenged revealed that both naïve and memory F5 CD8$^+$ T cells activated with cognate peptide or SEA sAg expanded to equivalent sized effector populations (Fig. 3g, h). Moreover, when we repeated the experiment above, but this time used endogenous memory Vβ8$^+$ influenza nucleoprotein (NP)-specific CD8$^+$ T cells purified from mice previously infected with influenza virus, we once again observed that Vβ8$^+$ NP-specific CD8$^+$ T cells activated with either sAg or cognate peptide recalled equivalently post influenza rechallenge (Fig S4). Together, these data show that sAg activation does not render naïve or memory T cells permanently dysfunctional, with both subsets mounting an intact recall response.

Local expansion of CD4$^+$ T cell in vivo following infection of DR4-DQ8 mice with sAg expressing S. aureus strains

We next evaluated the impact of sAgs on T cell function and fate, in vivo. To do this, sAg sensitive DR4-DQ8 mice, or as controls, sAg resistant B6 mice, were intranasally infected with 10^8 CFU of either parental JKD6159 or the SEB sAg expressing JKD6159::*seb*, and the size and functionality of the local and circulating T cell pools were profiled. Assessment of the levels of a panel of pro-inflammatory cytokines and chemokines in the serum and bronchial alveolar lavage fluid (BALF) 24 hrs post infection revealed that infection of DR4-DQ8 mice with the JKD6159::*seb* strain indeed triggered significantly higher levels of IFNγ and IFNβ in the BALF, and IFNγ in the serum, as compared to all other cohorts (Fig. 4a), confirming the ability of the sAg-expressing strains to trigger hyperinflammation.

Next, we checked whether infection with the SEB sAg-expressing strain of *S. aureus* caused polyclonal CD4$^+$ T cell expansion. As SEB sAg preferentially activates T cells expressing a Vβ8 TCR we quantitated the number of CD4$^+$Vβ8$^+$ T cells, and as a control non-SEB reactive CD4$^+$Vβ11$^+$ T cells, in the lung, mLN and spleen at days 2, 4 and 7 post infection. We observed no significant fluctuation over the course of the infection, in the number of CD4$^+$Vβ8$^+$ and CD4$^+$Vβ11$^+$ T cells in the spleen, lung, and mLN of B6 and DR4-DQ8 mice infected with JKD6159 strain or B6 mice infected with strain JKD6159::*seb* (Fig. 4b–d). In contrast, at day 4 post infection of DR4-DQ8 mice with the SEB sAg expressing strain (JKD6159::*seb*), a 100-fold increase in the number of lung CD4$^+$Vβ8$^+$ T cells was observed, while no significant elevation in the number of non SEB reactive CD4$^+$Vβ11$^+$ T cells were detected in this region (Fig. 4b, c). This boost in the CD4$^+$Vβ8$^+$ T cell pool following intranasal infection of DR4-DQ8 mice with JKD6159::*seb* was restricted to the lung tissue, as no preferential increase in the number of CD4$^+$Vβ8$^+$ T cells was observed in the mLN or spleen of these animals over the course of the infection (Fig. 4b, c).

While the SEB sAg preferentially activates Vβ8$^+$ mouse T cells, there are reports this sAg can also stimulate T cells expressing Vβ7 and Vβ3 TCR elements. To confirm that our approach to track Vβ8 T cells was capturing the bulk of the sAg activated T cell pool, we profiled the TCR Vβ usage of CD4$^+$ T cells in the spleen and lung of DR4-DQ8 mice on day 4 days post intranasal infection with JKD6159 or JKD6159::*seb*. Once again, only infection with the sAg expressing strain significantly altered the CD4 Vβ repertoire, this was limited to the lung, primarily resulting in the expansion of CD4$^+$ T cells expressing TCR Vβ8.1/2 and Vβ8.3 (Fig. 4e).

Assessment of the distribution of HLA-DR on cells in the lung of DR4-DQ8 mice revealed the majority of expression (>85%) was on B cells, and while both DCs and macrophages also express HLA-DR and do upregulate co-stimulatory molecules following infection with JKD6159::*seb* (Fig S5a, b), it is highly plausible that the majority of sAg stimulated CD4$^+$ Vβ8$^+$ T cells in the lung following JKD6159::*seb* infection were not activated by a professional antigen presenting cell, and therefore in the absence of effective co-stimulation. Hence, we next assessed whether the pool of CD4$^+$Vβ8$^+$ T cells in the lung of JKD6159::*seb* infected DR4-DQ8 were anergic. To do this, we infected DR4-DQ8 or B6 mice intranasally with 10^8 CFU of either parental JKD6159 or JKD6159::*seb* and on day 4 post infection we recovered the lungs and spleens and measured TNFα production by either bulk CD4$^+$ T cells, or Vβ8$^+$ or Vβ8$^-$ CD4$^+$ T cells following a brief in vitro stimulation with PMA and ionomycin. While a similar proportion of TNFα producing total, Vβ8$^+$ and Vβ8$^-$ CD4$^+$ T cells were detected in the spleens across all cohorts, in the lung, we observed a significant reduction in the proportion of TNFα$^+$ total CD4$^+$ T cells, and Vβ8$^+$ but not Vβ8$^-$ CD4$^+$ T cells exclusively in DR4-DQ8 mice infected with JKD6159::*seb* (Fig. 4f–h). To check the longevity of this anergic state, we repeated the experiment described above but measured CD4$^+$ T cell functionality at 2-, 7-, 14- and 21-days post infection. Interestingly, at day 2 post challenge, a timepoint prior to sAg induced Vβ8$^+$CD4$^+$ T cells expansion in the lung of DR4-DQ8 mice, we observe no impairment in the cytokine production of this T cell subset, which suggests functional impairment succeeds sAg induced expansion (Fig. S6a). While CD4$^+$Vβ8$^+$ T cells in the lung of JKD6159::*seb* infected DR4-DQ8 mice were still functionally impaired at day 7 post infection (Fig. S6b), at day 14 and 21 post infection, the lung Vβ8$^+$CD4$^+$ T cell subset had regained

https://doi.org/10.1038/s41467-024-54074-8

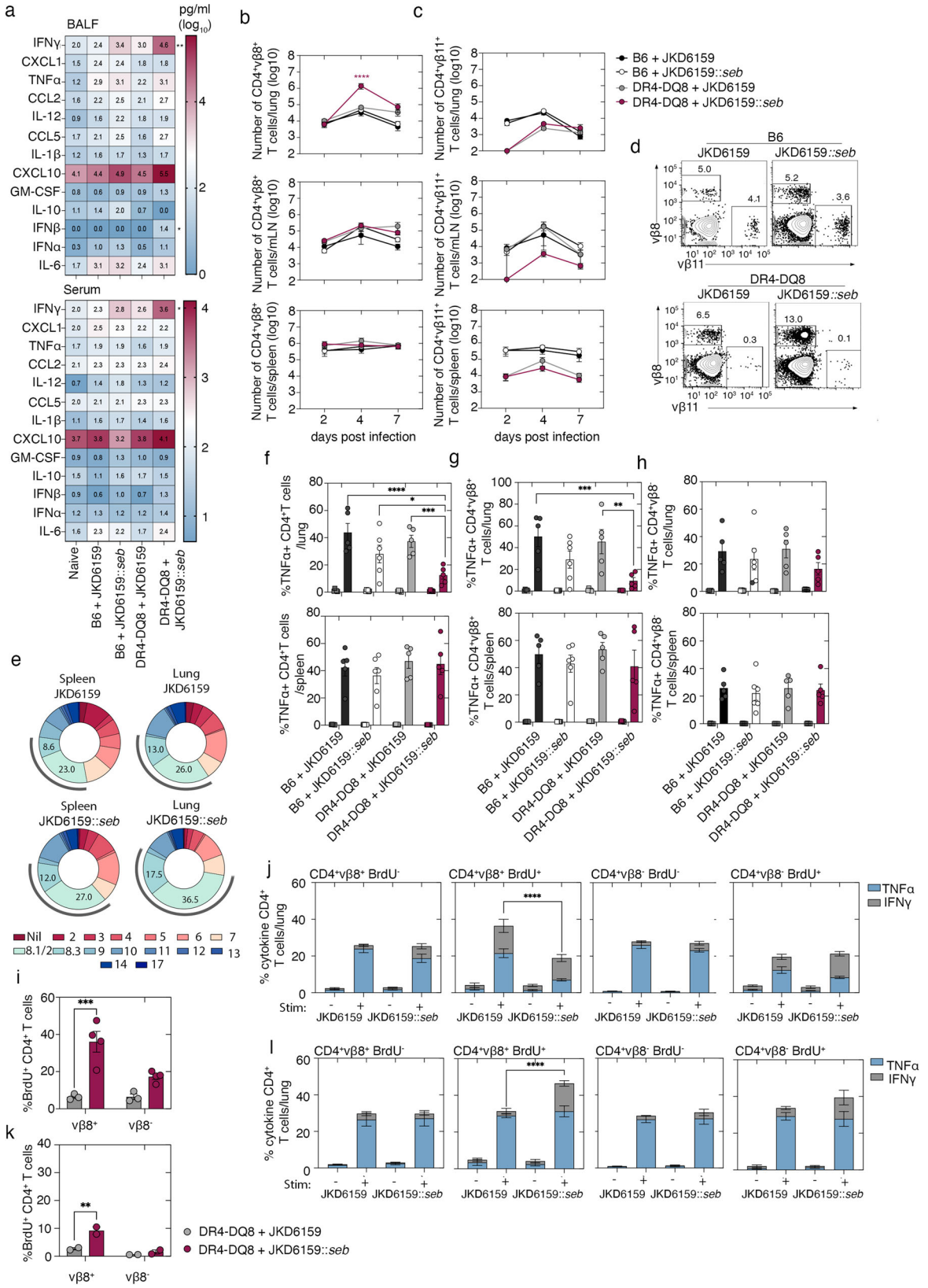

full effector function (Fig S6c, d). This defect in cytokine production was not limited to TNFα production as assessment of a larger panel of cytokines (IL-17, IFNγ, IL-2) revealed that Vβ8$^+$ CD4$^+$ T cells in the lung of DR4-DQ8 mice infected with JKD6159::*seb* failed to produce multiple cytokines (Fig S6e, f). To show that the functional impairment was reflective of the cells becoming anergic and not exhausted, we checked the cells for the levels of expression of exhaustion (Tigit, Tim-3, Lag3, PD-1) and anergy markers (CD73, FR4). Here we found that Vβ8$^+$ CD4$^+$ T cells in the lung of JKD6159::*seb* infected DR4-DQ8 mice expressed negligible levels of exhaustion markers at all time points, while by day 7 p.i. ~20% of Vβ8$^+$ CD4$^+$ T cells in the lung co-expressed the anergy markers, CD73 and FR4 (Fig. S7a–d). In contrast, <10% of Vβ8$^-$ CD4$^+$

Fig. 4 | Local expansion and transient and reversible anergy of CD4⁺ T cells following pulmonary infection with sAg expressing *S. aureus* strains. a C57BL/6 mice and DR4-DQ8 mice were intranasally infected with either 10^8 CFU JKD6159, or 10^8 CFU JKD6159::*seb*. On day 1 post infection, the concentration of a panel of cytokines in the BALF and serum was measured using a cytometric bead array ($n = 6–9$ mice per group, Two-way ANOVA, Dunnett's multiple comparison). **b–d** C57BL/6 mice and DR4-DQ8 mice were intranasally infected with either 10^8 CFU JKD6159, or 10^8 CFU JKD6159::*seb*. On days 2, 4 or 7 post infection, the absolute number of (**b**) Vβ8⁺CD4⁺ T cells (**c**) Vβ11⁺CD4⁺ T cells in the lung, mLN and spleen was measured by flow cytometry. The lines represent different experimental groups, and symbols represent the mean ± SEM ($n = 5–28$ mice per group, Two-way ANOVA, Sidak's multiple comparison). **d** Representative flow cytometry profiles gated on CD4⁺ T cells in the lung showing the proportion of cells expressing Vβ8 and Vβ11 on day 4 post infection. **e** Normalized frequencies of Vβ TCR for bulk CD4⁺ T cells in the lung and spleen compartment in DR4-DQ8 mice intranasally infected with either 10^8 CFU JKD6159 or 10^8 CFU JKD6159::*seb* at day 4 after infection. Data are pooled from 2 experiments. C57BL/6 mice and DR4-DQ8 mice were intranasally infected with either 10^8 CFU JKD6159, or 10^8 CFU JKD6159::*seb*. Four days later the proportion of (**f**) total CD4⁺ T cells (**g**) CD4⁺Vβ8⁺ T cells or (**h**) CD4⁺Vβ8⁻ CD4⁺ T cells in the lung and spleen producing TNFα following a brief in vitro stimulation with PMA/ION was measured by flow cytometry. Bars represent the mean ± SEM, and symbols represent individual mice (squares represent unstimulated control) ($n = 5$ or 6 mice cohort, Two-way ANOVA, Tukey's multiple comparison). **i–l** DR4-DQ8 mice intranasally infected with either 10^8 CFU JKD6159 or 10^8 CFU JKD6159::*seb* and treated with BrdU from days 1–3 post infection. The proportion of CD4⁺Vβ8⁺ T cells and CD4⁺Vβ8⁻ T cells in the lung on (**i**) day 6 and (**k**) day 21 post infection. Bars represent the mean ± SEM ($n = 2–4$ mice cohort). The proportion of CD4⁺ Vβ8⁺BrdU⁺ or BrdU⁻ T cells or CD4⁺Vβ8⁻BrdU⁺ or CD4⁺Vβ8⁻BrdU⁻ T cells in the lung on (**j**) day 6 or (**l**) day 21 producing IFNγ and/or TNFα following a brief in vitro stimulation with PMA/ION was measured by flow cytometry. Bars represent the mean ± SEM ($n = 5–7$ mice cohort, Two-way ANOVA, uncorrected Fisher's LSD). $^*p < 0.5$, $^{**}p < 0.01$, $^{***}p < 0.001$, and $^{****}p < 0.0001$.

T cells recovered from the lung of JKD6159::*seb* infected DR4-DQ8 mice co-expressed these anergy markers (Fig S7a–d).

To establish whether the restoration of effector function of Vβ8⁺CD4⁺ T cells in the lung of JKD6159::*seb* infected DR4-DQ8 mice was due to the reversal of the anergic state in sAg activated Vβ8⁺ CD4⁺ T cells or the outgrowth of a subpopulation of Vβ8⁺CD4⁺ T cells that had escaped the initial anergy induction, we infected DR4-DQ8 mice with either JKD6159 or JKD6159::*seb*, and administered BrdU on days 1–3 post infection to label all actively dividing cells. The proportion and functionality of BrdU⁺ Vβ8⁺ CD4⁺ T cells in the lung was measured during and after sAg induced anergy. On day 6 post infection, the proportion of BrdU⁺CD4⁺Vβ8⁺ T cells in the lungs of DR4-DQ8 mice infected with JKD6159::*seb* was 6-fold greater than the proportion detected in animals infected with the parental JKD6159 strain, which is reflective of the SEB sAg preferentially driving Vβ8⁺ T cell activation. Similar percentages of BrdU⁺CD4⁺Vβ8⁻ T cells were detected in the lungs of DR4-DQ8 mice infected with either strain of bacterium (Fig. 4i). We next tested the cytokine production of these T cell populations and found that following a brief in vitro stimulation, CD4⁺Vβ8⁺BrdU⁺ T cells in the lung of JKD6159::*seb* infected mice displayed signs of anergy, producing significantly lower levels of IFNγ and TNFα when compared to CD4⁺Vβ8⁺BrdU⁺ T cells recovered from the lungs of JKD6159 infected mice (Fig. 4j). Notably, CD4⁺Vβ8⁺BrdU⁻ T cells in the lungs of JKD6159::*seb* infected mice, which likely escaped sAg activation, were fully functional and produced similar levels of cytokines as the matched subset in the lung of JKD6159 infected mice (Fig. 4j). As expected, equivalent levels of cytokine production were detected in both BrdU⁺ and BrdU⁻ non-SEB reactive CD4⁺Vβ8⁻ T cells in the lungs of either JKD6159 or JKD6159::*seb* infected mice (Fig. 4j).

We next performed a similar analysis on day 21 post infection. Here we found that while the proportion of BrdU⁺ CD4⁺Vβ8⁺ T cells in the lungs of DR4-DQ8 mice infected with JKD6159::*seb* had reduced to 10% of total CD4⁺Vβ8⁺ T cells (Fig. 4k), assessment of the cytokine production of the residual BrdU⁺ CD4⁺Vβ8⁺ T cells in the lungs of these mice revealed no impairment, and in fact, CD4⁺Vβ8⁺BrdU⁺ T cells in the lungs of JKD6159::*seb* infected mice now produced significantly more cytokines than the matched subset recovered from the lungs of JKD6159 infected mice (Fig. 4 l). These data show that the anergic state of sAg expanded T cells is reversible and restoration of this effector function was in part, due to the reversal of the anergic state in sAg-activated T cells.

Fate and functionality of resident memory T cells in situ following pulmonary infection with sAg expressing S. aureus strains

Lung Trm cells play a critical role in the defence against respiratory pathogens[24]. As pulmonary infection with sAg expressing strains of bacterium alter the T cell landscape within the lung, we next tested the impact of sAg on bacterial-reactive, and sAg-reactive lung Trm. To this end, we used a previously established approach[25] to deposit Trm cells in the lung. We lodged in the lung of either B6 of DR4-DQ8.F1 mice SEB sAg responsive Vβ8 restricted SMARTA.CD90.1⁺ CD4⁺ Trm cells, as well as gDT-2.CD45.1⁺ CD4⁺ Trm (as determined by CD69 expression and i.v. antibody labelling), which are specific for the $gD_{315-327}$ epitope of herpes simplex virus 1 (HSV-1), and as we have previously shown, will respond to *S. aureus* strains engineered to express this $gD_{315-327}$ epitope[25] (Fig. 5a, b; Fig. S8a). Next, we infected these mice intranasally with either JKD6159-gD or JKD6159-gD::*seb* and 4 days later, we measured the size and functionality of the bacterium-specific gDT-2.CD45.1⁺ CD4⁺ T cells, the SEB reactive SMARTA.CD90.1⁺ CD4⁺ T cells, and additionally the endogenous CD4⁺Vβ8⁺ T cells and CD4⁺Vβ11⁺ T cells in the lung and spleen. Consistent with earlier results, we found that infection of DR4-DQ8.F1 mice with JKD6159-gD::*seb* caused the preferential expansion of endogenous CD4⁺Vβ8⁺ T cells, but not non-SEB reactive CD4⁺Vβ11⁺ T cells in the lung (Fig. 5c). This effect was not seen in the spleen and was not seen following infection with JKD6159-gD (Fig. 5c). While the number of bacterium-specific gDT-2.CD45.1⁺ cells in the lung and spleen at day 4 post infection were similar across all experimental cohorts, a clear elevation in the number of SMARTA.CD90.1⁺ CD4⁺ T cells was detected in the lung, but not the spleen of DR4-DQ8.F1 mice infected with JKD6159-gD::*seb* (Fig. 5d, e). We next checked the functionality of these cells following a brief in vitro stimulation and found that bacterium specific gDT-2.CD45.1⁺ CD4⁺ T cells in both the spleen and lung of all cohorts produced similar levels of TNFα. Thus, the sAg induced hyperinflammatory environment does not impair the functionality of bacterium-specific CD4⁺ T cells within this niche (Fig. 5f). Interestingly, while the endogenous CD4⁺Vβ8⁺ CD4⁺ T cells in the lungs of DR4-DQ8.F1 mice infected with JKD6159-gD::*seb* displayed signs of anergy and released significantly lower levels of TNFα following in vitro stimulation (Fig. 5h), the SMARTA.CD90.1⁺ CD4⁺ Trm cells recovered from the lung of this cohort of mice were fully functional and produced matched levels of TNFα to all other cohorts (Fig. 5g). Thus, bacterium specific lung CD4⁺ gDT-2.CD45.1⁺ Trm retain normal functionality even when recalled within a sAg induced hyperinflammatory environment, while sAg-reactive SMARTA.CD90.1⁺ CD4⁺ Trm are less sensitive to sAg induced functional anergy.

We next checked whether sAg exposure resulted in any long-term functional impairment of the lung Trm pool. To this end, we lodged F5.CD45.1⁺ CD8⁺ Trm cells (as determined by CD69 and CD103 co-expression and i.v. antibody labelling) in the lungs of DR4-DQ8.F1 mice (Fig. 5i, Fig. S8b) and infected these animals intranasally with either JKD6159 or JKD6159::*sea*. Infection of DR4-DQ8.F1 mice with the SEA sAg-expressing JKD6159::*sea* strain resulted in F5 Trm activation, as on day 4 post infection an increase in the total number of F5.CD45.1⁺ CD8⁺

https://doi.org/10.1038/s41467-024-54074-8

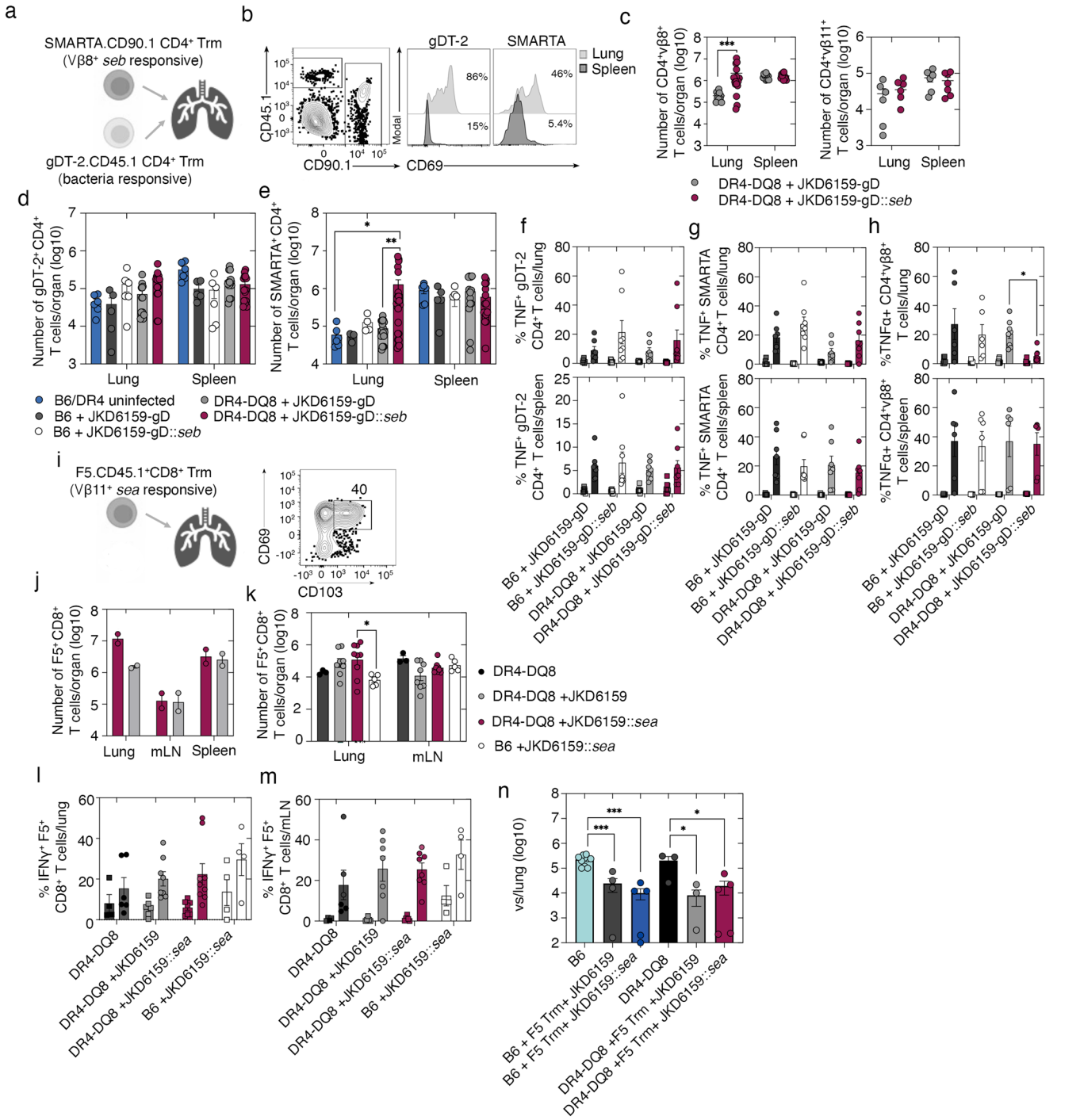

T cells in the lung, but not the mLN or spleen were observed in this cohort compared to animals infected with the parental JKD6159 strain (Fig. 5j). To test the long term impact sAg exposure has on lung F5.CD45.1$^+$ CD8$^+$ Trm, DR4-DQ8.F1 mice and as a control, B6 mice with lung F5.CD45.1$^+$ CD8$^+$ Trm left uninfected, or infected intranasally with JKD6159 or JKD6159::*sea* were challenged at day 15 post bacterial infection with X31(DAM) and the number and functionality of these influenza specific F5 CD8$^+$ T cell and their capacity to attenuate influenza virus infection was assessed. The total number of F5.CD45.1$^+$ CD8$^+$ T cells in the lung and mLN on day 4 post influenza virus infection and the capacity of these cell to make IFNγ was similar across all cohorts (Fig. 5k–m), again suggesting that sAg exposure does not have long term effects on the functionality of lung Trm. Moreover assessment of the viral loads in the lungs of either naïve B6 or DR4-DQ8.F1 mice, or cohorts of B6 or DR4-DQ8.F1 mice seeded with lung F5.CD45.1$^+$ CD8$^+$ Trm and infected with either JKD6159 or JKD6159::*sea*, and then challenged with X31(DAM) revealed that all cohorts of mice with lung F5.CD45.1$^+$ CD8$^+$ Trm, irrespective of whether these Trm had been exposed to SEA sAg, had 10-fold less influenza virus in the lung compared to the titres present in the naïve control mice (Fig. 5n). Collectively, these data show that sAg reactive lung Trm proliferate following pulmonary infection with sAg expressing bacteria, however these cells do not display signs of anergy or long-term functional impairment, maintaining the capacity to protect against pulmonary virus infections.

Fig. 5 | Lung resident memory T cells retain intact functionality following pulmonary infection with sAg expressing *S. aureus* strains. a DR4-DQ8.F1 mice seeded with 5×10^6 in vitro activated SMARTA.CD90.1 and 5×10^6 in vitro activated gDT-2.CD45.1 cells were intranasally immunised with 30 µg of $GP_{61\text{-}80}$ and $gD_{315\text{-}327}$ peptide and adjuvant and were rested for 15 days. **a** Schematic of experimental set up to lodge SMARTA and gDT-2 $CD4^+$ Trm in the lung of mice. Created in BioRender. Wakim, L. (2024) BioRender.com/w79t204. **b** Representative flow cytometry profiles show the level of expression of the Trm marker CD69 on SMARTA ($CD90.1^+$) and gDT-2 ($CD45.1^+$) cells in the lung and spleen on day 15 post seeding. Mice generated as described in (**a**) were intranasally infected with either 10^8 CFU JKD6159-gD, or 10^8 CFU JKD6159-gD::*seb* and spleen and lung were harvested 4 days later. **c** The absolute number of endogenous $CD4^+V\beta8^+$ and $CD4^+V\beta11^+$ T cells in the lung and spleen. Symbols represent individual mice, and the bars represent the mean ± SEM. Data pooled from 3 experiments. ($n = 5$–24 mice per group, Two-way ANOVA, Sidak's multiple comparison). **d**–**h** B6 and DR4-DQ8.F1 mice with SMARTA.$CD90.1^+$ and gDT-2.$CD45.1^+$ lung Trm (generated as described in a) were intranasally infected with either 10^8 CFU JKD6159-gD, or 10^8 CFU JKD6159-gD::*seb* and 4 days later the number of (**d**) gDT-2.$CD45.1^+$ and (**e**) SMARTA.$CD90.1^+$ $CD4^+$ T cells in the spleen and lung were measured. Symbols represent individual mice, and the bars represent the mean ± SEM. Data pooled from 5 experiments. ($n = 5$–24 mice per group, Two-way ANOVA, Sidak's multiple comparison). The proportion of (**f**) gDT-2.$CD45.1^+$ $CD4^+$ T cells (**g**) SMARTA.$CD90.1^+$ $CD4^+$ T cells or (**h**) endogenous $CD4^+V\beta8^+$ T cells in the lung and spleen producing TNFα following a brief in vitro stimulation was measured by flow cytometry. Bars represent the mean ± SEM, and symbols represent individual mice ($n = 6$–9 mice cohort, Two-way ANOVA, Tukey's multiple comparison). **i** DR4-DQ8.F1 mice seeded with 5×10^6 in vitro activated F5.$CD45.1^+$ $CD8^+$ T cells were intranasally immunised with 30 µg of $NP_{366\text{-}374}$ peptide and adjuvant and were rested for 15 days. Representative flow cytometry profile showing the proportion of F5.$CD45.1^+$ $CD8^+$ T cells in the lung expressing Trm markers, CD69 and CD103 on day 15 post seeding. Created in BioRender. Wakim, L. (2024) BioRender.com/w79t204. **j** Mice generated as described in **i** were intranasally infected with either 10^8 CFU JKD6159, or 10^8 CFU JKD6159::*sea* and spleen, mLN and lung were harvested 4 days later. (j) The absolute number of F5.$CD45.1^+$ $CD8^+$ T cells in the lung, mLN and spleen. Bars represent the mean ± SEM ($n = 2$). **k**–**n** B6 and DR4-DQ8.F1 mice with F5.$CD45.1^+$ $CD8^+$ lung Trm generated as described in (**i**) were intranasally infected with either 10^8 CFU JKD6159, or 10^8 CFU JKD6159::*sea* or left uninfected and 21 days later were intranasally challenged with 10^4 PFU of X31(DAM). **k** The absolute number of F5.$CD45.1^+$ $CD8^+$ T cells in the lung and mLN. Symbols represent individual mice, and the bars represent the mean ± SEM. Data pooled from 2 experiments. ($n = 3$-9, Two-way ANOVA, Sidak's multiple comparison). The proportion of F5.$CD45.1^+$ $CD8^+$ T cells in the (**l**) lung and (**m**) mLN producing IFNγ following a brief in vitro stimulation was measured by flow cytometry. Bars represent the mean ± SEM, and symbols represent individual mice ($n = 4$–9 mice cohort, Two-way ANOVA, Tukey's multiple comparison). **n** B6 or DR4-DQ8.F1 mice with F5.$CD45.1^+$ $CD8^+$ lung Trm (generated as described in i) were intranasally infected with either 10^8 CFU JKD6159, or 10^8 CFU JKD6159::*sea* or left uninfected. Fifteen days later, these animals, in addition to a cohort of naïve DR4-DQ8.F1 and B6 mice were infected intranasally with 10^4 PFU X31(DAM) and viral loads in the lung on day 4 post influenza infection were measured. Bars represent the mean ± SEM, and symbols represent individual mice ($n = 4$–9 mice cohort, Two-way ANOVA, Tukey's multiple comparison). *$p < 0.5$, **$p < 0.01$, ***$p < 0.001$, and ****$p < 0.0001$.

An intact bacterium specific $CD4^+$ T cell response can be mounted in the face of sAg induced immune hyperactivation

Bacteria secreted sAgs are assumed to obstruct the development of a pathogen specific cellular immune response. To check whether sAg induced hyperimmune activation impacts priming of a bacterium specific $CD4^+$ T cell response, we seeded DR4-DQ8.F1 mice or as a control, B6 mice with 1×10^6 CFSE-labelled naïve gDT-2.$CD45.1^+$ $CD4^+$ T cells and intranasally infected these animals with either JKD6159-gD or JKD6159-gD::*seb* and the number of divided bacterium specific gDT-2.$CD45.1^+$ $CD4^+$ T cells in the cLN, mLN and spleen was measured 4 days later. The absolute number of divided gDT-2.$CD45.1^+$ $CD4^+$ T cells in all lymphoid compartments was comparable across all cohorts, which suggests a localised infection with a sAg-expressing bacterium does not block the priming of bacterium-specific $CD4^+$ T cell response (Fig. 6a–d). We next checked whether this was also the case following a systemic bacterial infection. We seeded B6 or DR4-DQ8.F1 mice with violet trace-labelled gDT-2.$CD45.1^+$ $CD4^+$ T cells, and infected these animals intravenously with JKD6159-gD or JKD6159-gD::*seb*. Firstly, we confirmed infection of DR4-DQ8.F1 mice with SEB expressing strains of bacteria via the intravenous route significantly elevated the levels of pro-inflammatory cytokines in the serum when compared to the levels present in the serum of either naïve mice or DR4-DQ8.F1 mice infected with non-sAg expressing strains (Fig. 6e). Next, we showed that on day 4 post infection, both DR4-DQ8.F1 and B6 mice infected with either JKD6159-gD or JKD6159-gD::*seb* had equivalent bacterial loads in the lung, liver, kidney and spleen, (Fig. 6f) and importantly, the number of divided gDT-2.$CD45.1^+$ cells in the kidney draining LN, spleen and mLN were comparable across all cohorts of mice (Fig. 6g). Moreover, following a brief restimulation with their cognate peptide, divided gDT-2.$CD45.1^+$ $CD4^+$ T cells in the spleen of all cohorts made similar levels of TNFα (Fig. 6h–i). Thus, systemic infection with a sAg expressing bacterium does not block the priming or impact the functionality of bacterium specific $CD4^+$ T cells. Assessment of the number and functionality of endogenous SEB reactive $CD4^+V\beta8^+$ T cells in these cohorts did show a significant elevation of this subset in the spleen of DR4-DQ8.F1 mice infected intravenously with JKD6159-gD::*seb* strain, but not JKD6159-gD (Fig. 6j). Moreover, $CD4^+V\beta8^+$ T cells in the spleen of DR4-DQ8.F1 mice infected with JKD6159-gD::*seb* strain showed signs of anergy, producing significantly lower levels of TNFα when compared to the matched subset in the spleen of DR4-DQ8.F1 mice infected with a non-sAg-expressing bacterium (Fig. 6k). Again, the functionality of non-SEB reactive T cells ($CD4^+V\beta8^-$) remained intact across both cohorts.

Finally, we checked whether the presence of sAgs could impair the functionality and recall capacity of bacterium-specific memory $CD4^+$ T cells. To do this, we seeded B6 or DR4-DQ8.F1 mice with naive gDT-2.$CD45.1^+$ $CD4^+$ T cells, infected these animals intravenously with JKD6159-gD or JKD6159-gD::*seb* and 28 days later animals were intranasally infected with an influenza virus engineered to express the gD epitope (X-31-gD). The number of gDT-2.$CD45.1^+$ $CD4^+$ T cells in the lung, mLN and spleen and their cytokine profile were measured 7 days later. Here we found that bacterium-specific gDT-2.$CD45.1^+$ $CD4^+$ T cells activated the presence or absence of sAg-induced hyperinflammation underwent equivalent levels of recall expansion, with similar numbers of gDT-2.$CD45.1^+$ $CD4^+$ T cells being detected in the mLN, spleen and lung across all cohorts (Fig. 6l–n). Then, following a brief in vitro stimulation, gDT-2.$CD45.1^+$ $CD4^+$ T cells recovered from the lung and mLN of all cohorts produced similar levels of IFNγ (Fig. 6o, p). Thus, using both a localised and systemic bacteraemia model, we provide evidence that bacterium-secreted sAgs do not interfere with the activation, functionality, and memory development of pathogen-specific $CD4^+$ T cells.

Discussion

sAgs are bacterial virulence factors that induce a state of immune hyperactivation by cross-linking the TCR and MHC class II molecules, triggering uncontrolled activation of T lymphocytes, cytokine storm and toxic shock. The acute and long-term outcomes of this exposure on sAg responsive, and bacteria reactive T cell function and fate remains unclear. In the current study, using sAg sensitive human MHC-II transgenic mice and a panel of sAg producing *S. aureus* strains engineered to express trackable $CD4^+$ T cell epitopes, we show that post exposure, sAg responsive T cells are not rendered permanently dysfunctional and regain full effector function following a transient and reversible anergy. Moreover, we demonstrate that an intact bacteria-reactive T cells response can be mounted in the face of sAg induced immune hyperactivation.

https://doi.org/10.1038/s41467-024-54074-8

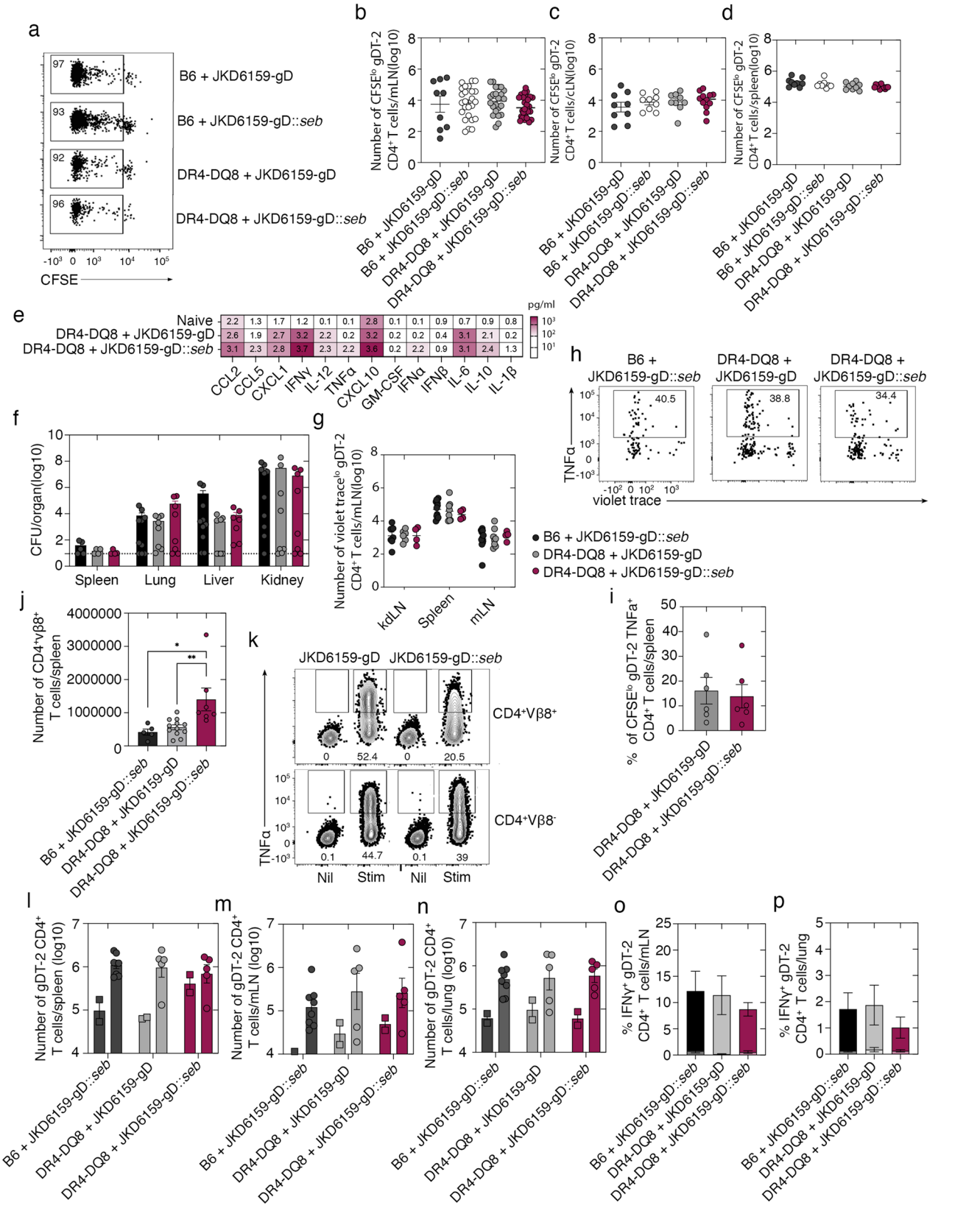

While the capacity of sAgs to trigger aberrant and widespread T cell activation and hypercytokinemia is well-established[2–5], there is conflict as to whether this stimulation incapacitates and deletes T cells, or whether T cells regain normal functionality post sAg exposure. While several reports indicate that T cells become anergic following exposure to sAgs and that certain Vβ subsets can be reduced or deleted[26–29], an equal number of studies report that sAg exposure causes no long term impairment of the T cell repertoire[30–32]. Moreover, while it is reported that memory T cells are more sensitive to sAg induced deletion and/or anergy[28,29], others studies show that bacterial sAgs do not delete, and instead, expand and activate antigen experienced memory T cells[31]. Several of abovementioned studies were

Fig. 6 | An intact bacterium specific CD4⁺ T cell response can be mounted in the face of sAg induced immune hyperactivation. C57BL/6 mice and DR4-DQ8.F1 mice seeded with 1×10^6 CFSE labelled gDT-2.CD45.1⁺ CD4⁺ T cells were intranasally infected with either 10^8 CFU JKD6159-gD, or 10^8 CFU JKD6159-gD::*seb* and the proportion of divided ($CFSE^{lo}$) gDT-2.CD45.1⁺ CD4⁺ T cells in the mLN, cLN and spleen were measured by flow cytometry. **a** Representative flow cytometry profiles gated on gDT-2.CD45.1⁺ CD4⁺ T cells in the mLN on day 4 post infection showing the proportion of $CFSE^{lo}$ cells. The absolute number of divided gDT-2 CD4⁺ T cells in the (**b**) mLN (**c**) cLN, (**d**) spleen on day 4 post infection. Symbols represent individual mice, and the bars represent the mean ± SEM. Data pooled from 5 experiments. **e**–**k** C57BL/6 mice and DR4-DQ8.F1 mice seeded with 1×10^6 violet trace labelled gDT-2.CD45.1⁺ CD4⁺ T cells were intravenously infected with either 10^6 CFU JKD6159-gD or 10^6 CFU JKD6159-gD::*seb* (**e**). The concentrations of a panel of cytokines and chemokines in the serum was measured 24 hrs post infection. **f** The bacterial loads in the spleen, lung, liver and kidney were measured on day 4 post infection. Bars represent the mean ± SEM, and symbols represent individual mice. Dotted line depicts the limit of detection. Data pooled from 2 experiments ($n = 5$–10 mice). **g** The absolute number of divided (violet $trace^{lo}$) gDT-2.CD45.1⁺ CD4⁺ T cells in the spleen, kdLN and mLN were measured by flow cytometry. Symbols represent individual mice, and the bars represent the mean ± SEM. Data pooled from 3 experiments ($n = 4$–8). **h** Representative flow cytometry profiles gated on gDT-2.CD4.1⁺ T cells in the spleen, showing the proportion of cells producing TNFα following a brief in vitro stimulation with $gD_{315\text{-}327}$ peptide (**i**). Graphs shows the percentage of divided gDT-2 CD4⁺ T cells producing TNFα in the spleen. Symbols represent individual mice, and the bars represent the mean ± SEM. Data pooled from 2 experiments ($n = 6$). **j** Graph shows the absolute number of endogenous CD4⁺Vβ8⁺ T cells in the spleen on day 4 post infection. Data pooled from 3 experiments. Symbols represent individual mice, and the bars represent the mean ± SEM ($n = 4$–12 mice; one-way ANOVA, Tukey's multiple comparison). **k** Representative flow cytometry profiles gated on endogenous CD4⁺Vβ8⁺ or CD4⁺Vβ8⁻ T cells in the spleen, showing the proportion of cells producing TNFα following a brief in vitro stimulation with PMA/ION. **l**–**n** C57BL/6 mice and DR4-DQ8.F1 mice seeded with 1×10^6 violet trace labelled gDT-2.CD45.1⁺ CD4⁺ T cells were intravenously infected with either 10^6 CFU JKD6159-gD or 10^6 CFU JKD6159-gD::*seb* and 28 days later mice were infected intranasally with 10^4 PFU X-31-gD. The absolute number of gD-2.CD45.1⁺ CD4⁺ T cells in the (**l**) spleen, (**m**) mLN and (**n**) lung on day 7 post influenza infection. Symbols represent individual mice (squares represent control cohorts not infected with influenza virus). Bars represent the mean ± SEM. Data pooled from 2 experiments ($n = 2$–8 mice cohort) (**o**–**p**) the proportion of gDT-2.CD4⁺ T cells producing IFNγ in the (**o**) mLN and (**p**) lung on day 7 post infection directly ex vivo (non-shaded bars) or following a brief in vitro restimulation (shaded bars). Bars represent the mean ± SEM. Data pooled from 3 experiments ($n = 6$ mice cohort). $^*p < 0.5$, $^{**}p < 0.01$, $^{***}p < 0.001$, and $^{****}p < 0.0001$.

performed in sAg-insensitive mouse strains which require the administration of a large bolus of purified toxin to trigger hyperimmune activation, therefore T cell fate post sAg exposure reported in these studies may be affected by the use of non-physiological doses of the toxin. Using sAg-sensitive humanised HLA-DR4 mice we profiled T cell fate using a physiologically relevant infection model where we challenged these animals with sAg expressing *S. aureus* strains. We demonstrated that sAg activation does not render CD4⁺ T cells permanently dysfunctional, and full restoration of effector function is observed following a transient anergy. Interestingly, by permanently tagging sAg-activated CD4⁺ T cells during their initial clonal expansion, we could explore whether the restoration of effector function of sAg-activated CD4⁺ T cells in vivo was due to the reversal of the anergic state, or the outgrowth and replacement of this T cell pool by a subpopulation of T cells that had escaped the initial anergy induction. We show that a proportion of Vβ8⁺CD4⁺ T cells which non-specifically expand in situ in the lung in response to a pulmonary infection with a SEB sAg expressing strain of *S. aureus* and displayed signs of functional anergy at one week post infection, regained full effector function by three weeks post infection. While we show that the anergic state of sAg expanded T cells is reversable, further studies are warranted to dissect whether this is achieved through the autonomous restoration of T cell effector function, or as proposed by earlier works[33], the decay of sAg induced suppressor cells which are responsible for actively maintaining sAg induced anergy.

sAgs are proposed to be produced by bacteria as a defence mechanism against the host's immune system and serve to circumvent the development of a pathogen specific cellular immune response by creating an immunological 'smoke screen'[34]. Our findings challenge the dogma that sAgs are produced by bacteria simply as an immunological diversion. Here, using a panel of sAg producing *S. aureus* strains we engineered to express trackable CD4⁺ T cell epitopes, we provide evidence that during a natural infection, bacterium-secreted sAgs do not interfere with the activation, functionality and memory development of bacteria specific CD4⁺ T cells. Our results are reflective of several observations from human studies that clearly show the high prevalence of *S. aureus* antigen-specific circulating[35] and tissue bound[25,36] memory CD4⁺ T cells, despite the ubiquity of sAgs in clinical *S. aureus* isolates. Moreover, the high frequency of neutralising antibodies against *S. aureus* sAgs[37–39], further implies that the CD4⁺ T cell helper compartment is functional during and after *S. aureus* infection even when sAgs are expressed. These data would suggest that sAg-induced T cell hyperactivation does not serve to directly obstruct the development of a pathogen specific T cell response. So, what is the evolutionary benefit bacteria gain from producing such powerful T cell mitogens? An elegant study by Tuffs et al.[40], shed light on how these toxins manipulate the immune system to facilitate bacterial colonisation. They show that sAg induced CD4⁺ T cell hyperactivation resulted in the release of pathogenic levels of IFNγ which enhanced disease severity and bacterial burden in the liver by perturbing local macrophage activity. Although sAgs directly target T cells, the ultimate consequence may not be a debilitated immune cell population, but rather a strategy to evoke rapid hyper inflammation to subvert the activation and recruitment of innate immune cells. This inflammation would be consequential, as such myeloid cells are key players in the immediate defence against these bacteria.

The pathogenicity of sAg is due to the extraordinary ability of these toxins to trigger a cytokine storm, which can lead to hypotension, multiple organ failure and toxic shock. sAgs mediate their pathological effects by bridging major histocompatibility complex (MHC) class II and TCR to provoke aberrant T cell activation and cytokine release. The ability to inhibit the cytokine cascade early appears to be critical in mitigating the toxicity of bacterial sAgs. This remains a challenge, as many pharmacological interventions aimed to dampen the hyperimmune activation and block the ensuing cytokine storm, also cripple the development of a pathogen directed immune response, thus limiting the body's innate ability to rid itself of the invading pathogen orchestrating this disease. Here we show that the fate and responsiveness of T cells following sAg exposure is influenced by the maturity and location of the T cell population. Our in vitro experiments demonstrated that while naïve and central memory CD4⁺ and CD8⁺ T cell subsets proliferated following sAg exposure and released minimal cytokines, effector memory T cells failed to expand, and instead, hyper released pro-inflammatory cytokines. Thus, refined therapeutic strategies that exclusively block cytokine production by Tem cells may serve to attenuate the sAg-induced cytokine storm, while sparing other aspects of the immune response. Voltage-gated $K_V1.3$ channel inhibitors which are being developed as a clinical treatment for autoimmune conditions[18,19] have been reported to preferentially target Tem cells[20–22], reducing their expansion and cytokine production. Here we show, using an in vitro culture model that Vm24, a selective Kv1.3 inhibitor, can attenuate sAg induced cytokine release from human memory CD4⁺ T cells without altering activation. Whether these drugs have a therapeutic application in the treatment of

sAg-induced cytokine storm in vivo will need to be addressed in future studies.

sAg-expressing strains of bacteria cause severe morbidity and mortality worldwide. While such bacteria command an impressive armoury of virulence factors, those that interfere with the host's immune system significantly worsen disease outcomes. Greater understanding of the impact of sAgs on the fate and long-term functionality of different immune cells and the establishment of bacterium specific immunological memory will inform the development of refined therapeutic strategies to mitigate the toxicity and impact sAgs have on host immunity, effectively disarming these bacteria without debilitating the immune system.

Methods

Ethics statement

All animal experiments were conducted in accordance with the Institutional Animal Care and Use Committee guidelines of the University of Melbourne and were approved by the University of Melbourne AEC (AEC 2015181; 27205). Human experimental work was conducted according to the Declaration of Helsinki Principles and to the Australian National Health and Medical Research Council (NHMRC) Code of Practice. PBMCs from adult donors were isolated from buffy packs obtained from the Australian Red Cross Life Blood (West Melbourne, Australia). PBMCs were isolated by Ficoll-Paque density-gradient centrifugation and cryopreserved as previously described[41,42]. All experiments were performed in accordance with the Institutional Human Ethics Committee guidelines of the University of Melbourne and were approved by the University of Melbourne Human Ethics Committee (13908).

Mice

Female (6–14-week-old) C57BL/6 (CD45.2), gDT-2.CD45.1 (Vα3.2/Vβ2)[43], SMARTA.Thy1.1 (Vα2.3/Vβ8)[44], F5.CD45.1(Vα4/Vβ11)[45,46], HLA-DR4-DQ8[11] humanized transgenic mice lacking endogenous mouse MHC-II on a C57BL/6, DR4.DQ8F_1 [HLA-DR4-DQ8 x C57BL/6], mice were bred in-house and housed in specific pathogen-free conditions in the Biological Research Facility (BRF) at the Doherty Institute for Infection and Immunity, the University of Melbourne. All mouse strains used were shown not to carry *S. aureus*. All mice were kept in HEPA filtered, individually ventilated cages, with environmental enrichment, 12 h light dark cycle and food and water *ad libitum*.

Virus infections

Mice were infected intranasally in a volume of 30 µl with 10^4 PFU of either influenza X-31(DAM)[17] (H3N2 reassortant virus bearing the HA and neuraminidase genes from A/Aichi/2/1968 and the remaining six internal genes from PR8 which carries an $NP_{372-374}$ epitope sequence of the E61-13-H17 influenza strain. The "DAM" refers to the last 3 amino acids of the $NP_{372-374}$ epitope which were mutated to "DAM" from "ETM" in the WT X31) X-31 parental strain (H3N2) or X-31-gD. The X-31-gD virus is a H3N2 reassortant virus bearing the HA and neuraminidase genes from A/Aichi/2/1968 and the remaining six internal genes from PR8 and encodes the $gD_{315-327}$ peptide fragment of the HSV-1 glycoprotein D (IPPNWHIPSIQDA) within the neuraminidase stalk, inserted 193 bp after the gene start site. Thirteen non-essential amino acids of the NA gene were removed at the insertion point and viruses were sequenced to confirm the insertion of the $gD_{315-327}$ epitope into the NA.

Preparation of S. aureus for inoculation and collection of bacterial supernatants

Streptomycin resistant clones of each *S. aureus* were grown as previously described[47]. Mice were inoculated intranasally with 10^8 CFU of *S. aureus* in a volume of 30 µl or infected intravenously with 10^6 CFU of *S. aureus* in a volume of 200 µl. In some experiments mice were treated with 0.4 mg bromodeoxyuridine (BrdU) intranasally and intraperitoneally on days 1–3 post infection.

Bacterial supernatants were collected from overnight cultures of bacteria grown in brain heart infusion broth (BHI, Difco) with 100 µg/mL streptomycin (Sigma) at 37 °C in a shaking incubator (240 rpm), filtered through the 0.2 µm filter (Millipore), and stored at −20 °C.

Enumeration of bacterial and viral loads

To evaluate *S. aureus* bacterial loads, tissue was harvested into 1 ml PBS, homogenized and serial dilutions of organ homogenates were made in PBS, plated onto BHI agar plates containing 100 µg/ml streptomycin, and incubated overnight at 37 °C. To evaluate influenza virus load, lung tissue was harvested into 1 ml PBS, homogenized viral loads were measured using a ViroSpot assay as previously described[17].

Construction of sAg expressing and deficient *S. aureus* strains

The method of Monk and Stinear[48] was followed for the introduction of the sAg *sea* or *seb* onto the chromosome of JKD6159/JKD6159-gD or the deletion of *seb* and *seq/sek* from COL^{STR}. For JKD6159, the pKOR1 constructs were passaged through *Escherichia coli* IM93B or *E. coli* IM08B for COL[49,50]. For the introduction of *sea* or *seb* into $JKD6159^{STR}$ the equivalent location of *sea* on chromosome of the *S. aureus* strain Newman was chosen. Unexpectedly, no Sea activity was detected in vivo (but functional in vitro) from JKD6159::P*sea-sea*. In vivo Sea activity was restored when the promoter region from P*seb* was used (JKD6159::P*seb-sea*; called JKD6159::*sea*) to drive *sea* expression. Primers used are detailed in Supplementary Table 1.

Deletion constructs for Δ*seb* (IM1501/IM1502 and IM1503/IM1504) or Δ*seq/sek* (IM1601/IM1602 and IM1603/IM1604) were amplified from COL genomic DNA and then joined by Splice overlap extension (SOE) PCR with the outer two primers (IM1501/IM1504 or IM1601/IM1604) and cloned into pKOR1.

To introduce *sea* or *seb*, upstream and downstream flanks were amplified from JKD6159 genomic DNA and the superantigen genes amplified from either Newman genomic DNA (*sea* UP: IM1495/IM1496, *sea* DOWN: IM1499/IM1500, P*sea-sea*: IM1497/IM1498) or COL genomic DNA (*seb* UP: IM1495/IM1496, P*seb-seb*: IM1505/IM1506, *seb* DOWN: IM1507/IM1500). The three corresponding amplimers for each construct were joined by SOE-PCR and cloned into pKOR1 yielding pKOR1(P*sea-sea*) and pKOR1(P*seb-seb*). To replace P*sea* promoter with the P*seb* promoter, both the above plasmids were first digested with KpnI, then the UP-P*seb* was amplified with IM1495/IM1599 and the *sea*-DOWN was amplified with IM1600/IM1500. Both amplimers were joined by SOE-PCR and cloned into pKOR1 yielding pKOR1(P*seb-sea*).

Assessment of cytokines via cytometric bead array

Cytokine/chemokine concentrations in cell culture supernatants, bronchial alveolar lavage fluid, or serum was measured using a LegendPlex mouse antiviral response cytometric bead array (Biolegend) or BD Biosciences Mouse Th1/Th2/Th17 CBA kit, following manufacturer's instructions.

Purification and adoptive transfer of naive murine T cells

$CD4^+$ T cells isolated gDT-2.CD45.1, SMARTA.Thy1.1 or $CD8^+$ T cells isolated from F5.CD45.1 mice were purified from single cell suspensions prepared from lymph nodes (LN) and spleen through negative selection using previously described protocols[51]. Mice received 1×10^6 CFSE labelled naïve gDT-2 CD45.1 cells intravenously in a volume of 200 µl. Divided cells, termed $CFSE^{lo}$, were defined as any cell undergoing ≥1 cell division.

Generation of mice with T cell memory

Circulating memory. F5.CD45.1 $CD8^+$ T cells or SMARTA.Thy1.1 $CD4^+$ T cells were activated in vitro with 10^{-6}M $NP_{366-374}$ (ASNENMDAM) peptide or 10^{-6}M GP_{61-80} (GLKGPDIYKGVYQFKSVEFD) peptide pulsed

splenocytes, respectively as previously described[52]. Mice were injected intravenously with 1×10^7 in vitro activated effectors and rested for at least 10 days to establish circulating memory T cells. Transgenic memory T cells were enriched from the spleen and LN and then sort purified into Tem ($CD44^+CD62L^-$) and Tcm ($CD44^+CD62L^+$) subsets.

Lung resident memory. Mice were injected intravenously with 5×10^6 in vitro activated effectors (gDT-2.CD45.1 or F5.CD45.1 or SMARTA.Thy1.1) and at day 0 and 7 post transfer mice were administered intranasally 1 µg lipopolysaccharide (LPS) with 30 µg of cognate peptide in a volume of 30 µl and rested for at least 10 days.

Purification and adoptive transfer of sAg activated murine T cells

Naïve F5.CD45.1 enriched from the spleen and LN (as described above) or memory F5.CD45.1 $CD8^+$ T cells purified from mice with circulating memory (generated as described above) were cultured 1:1 with splenic DCs enriched from DR4-DQ8.F1 mice with either 10^{-6}M $NP_{366\text{-}374}$ (ASNENMDAM) peptide or 0.1% v/v bacterial supernatant collected from overnight cultures of JKD6159::*sea* in complete RPMI [10% FBS, 2 mM glutamine, 50 mM 2-β mercaptoethanol (2-ME), penicillin (100 U/ml), and streptomycin (100 µg/ml)]. Cultures were split 1:2 and were supplemented with 25 U/ml of IL-2 on days 2 and 3 of culture. On day 4 post culture 5×10^6 effector cells were intravenously transferred into naïve recipient mice which were rested for 10 days prior to challenge.

Flow cytometry and intracellular cytokine staining

Single-cell suspensions were prepared from the spleen and LN by mechanical disruption. Mice were perfused with PBS before the harvest of the lung tissue, which were then enzymatically digested for 1 h at 37 °C in 3 ml of collagenase type 3 (3 mg/ml in RPMI 1640 medium supplemented with 2% fetal bovine serum (FBS)). Cells were incubated with the appropriate cocktail of monoclonal antibodies (mAbs) for 30 min on ice. For intracellular cytokine analysis, single-cell suspensions of the lung and spleen were stimulated with either the 1 µM of cognate peptide ($NP_{366\text{-}374}$ (ASNENMDAM); $GP_{61\text{-}80}$ (GLKGPDIYKGVYQFKSVEFD); $gD_{315\text{-}327}$ (IPPNWHIPSIQDA)) or Phorbol myristate acetate (PMA) and ionomycin for 5 h at 37 °C/10% CO_2 in the presence of GolgiPlug (BD Biosciences) in complete RPMI [10% FBS, 2 mM glutamine, 50 mM 2-β mercaptoethanol (2-ME), penicillin (100 U/ml), and streptomycin (100 µg/ml)]. Cells were then surface stained for 30 min on ice with the appropriate mixture of mAbs and then intracellularly stained using a Foxp3 fix/perm kit (Thermo Fisher Scientific) according to the manufacturer's protocol. The conjugated mAbs obtained from BD Pharmingen, BioLegend, or eBioscience include mouse: anti-CD8 (53–6.7), anti–CD45.1 (A20), CD45.2 (104), anti-Vβ8.3(1B3.3), anti-Vβ11 (KT11), anti-CD44 (1M7), anti-CD103 (2E7), anti-CD69 (H1.2F3), anti–IFNγ (XMG1.2), anti–TNFα (MP6-XT22), anti-IL-17 (TC11-18H10.1), anti-IL-2 (JES6-5H4), anti-CD62L (MEL-14), anti-CD4 (GK1.5), anti-90.1 (OX.7), anti-PD-1 (RMP1-30), anti-Tigit (1G9), anti-Lag3 (C9B7W), anti-Tim3 (RMT3-23), anti-CD73 (TY/11.8), anti-FR4 (TH6), anti-B220 (RA3-6B2), anti-CD11c (N418), anti-F4/80(BM8), anti-CD80 (1PE(6-10A1)), anti-CD86 (PO3), anti-CD3 (17A2), anti-I-A/I-E (M5/114.15.2) and human: anti-CD69(FN50), anti-HLA-DR(L243), anti-CD45RA(HI100), anti-CD27(M-T271) anti-CD4(RPA-T4), anti-Kv1.3 (KCNA3), anti-TNF (MAb11), anti-IFNγ (4S.B3). Dilutions included in Supplementary Table 2. Vβ-usage analysis was performed using a BD Mouse Vβ TCR Screening Panel Kit (BD Biosciences, San Diego, CA, USA) according to the manufacturer's instructions. Intracellular BrdU staining was performed using a BD BrdU staining kit (BD Biosciences, San Diego, CA, USA) according to the manufacturer's instructions. Samples were acquired using a Becton Dickinson LSRFortessa flow cytometer, and data were analyzed using the FlowJo 10.10.0 software package (Tree Star Inc., Ashland, OR, USA).

Stimulation of human T cells with sAg containing bacterial supernatant

Monocyte derived DCs (moDCs) were differentiated from PBMCS as previously described[25]. 20,000 violet trace labelled moDCs or sort purified $HLA\text{-}DR^+$ cells were cultured 1:1 with CFSE labelled autologous unfractionated PBMCs or sort purified $CD4^+$ Tcm ($CD27^+CD45RA^-$), Tem ($CD27^-CD45RA^-$) and Tn ($CD27^+CD45RA^+$) for 7 days either alone, or with 0.1%, 1% and 10% v/v of bacterial supernatants harvested from overnight cultures of *S. aureus* strains in complete RPMI [10%] FBS, 2 mM glutamine, 50 mM 2-β mercaptoethanol (2-ME), penicillin (100 U/ml). After 7 days, the cultures were restimulated with the same strains of bacterial supernatant for 1 h at 37 °C/10% CO_2. Cells were subsequently cultured for an additional 4 h in the presence of GolgiPlug (BD Biosciences) in complete RPMI before flow cytometry staining. In some experiments 1 nM Vm24 toxin (alomone labs) was added to the culture to block Kv1.3 channel.

Stimulation of mouse T cells with sAg containing bacterial supernatant

Dendritic cells were enriched from enzymatically digested spleens collected from either B6 or DR4-DQ8 mice as previously described[51]. 50,000 DCs were cultured 1:1 or 2:1 with violet trace labelled $CD4^+$ T cells or $CD8^+$ T cells (enriched from either naïve SMARTA.Thy1.1, F5.CD45.1, or C57BL/6 mice or sort purified memory subsets) for 4 days either alone, or with 0.1%, 1% and 10% v/v of bacterial supernatants harvested from overnight cultures of *S. aureus* in complete RPMI [10%] FBS, 2 mM glutamine, 50 mM 2-β mercaptoethanol (2-ME), penicillin (100 U/ml). At various time points post culture, cells were restimulated with the same strains of bacterial supernatant for 1 h at 37 °C/10% CO_2. Cell were left for an additional 4 h in the presence of GolgiPlug (BD Biosciences) in complete RPMI before surface staining for 30 min on ice with the appropriate mixture of mAbs and then intracellularly stained using a Foxp3 fix/perm kit (Thermo Fisher Scientific) according to the manufacturer's protocol.

Statistical analysis

Comparison between two study groups was statistically evaluated by unpaired two-tailed *t* test or Mann–Whitney test. Comparison between more than two groups (single factor) were evaluated using one-way analysis of variance (ANOVA) with Tukey's or Dunnett's multiple comparison. Two-way ANOVA with Sidak's or multiple comparison on log10-transformed values was used to evaluate more than two groups at different time points. In all tests, statistical significance was quantified as $^*p < 0.5$, $^{**}p < 0.01$, $^{***}p < 0.001$, and $^{****}p < 0.0001$. Statistical analysis was performed using GraphPad Prism 10 software.

Reporting summary

Further information on research design is available in the Nature Portfolio Reporting Summary linked to this article.

Data availability

The authors declare that the data supporting the findings of this study are available within the paper and its supplementary information files or from the corresponding author upon request. Source data are provided with this paper.

References

1. Fraser, J. D. & Proft, T. The bacterial superantigen and superantigen-like proteins. *Immunol. Rev.* **225**, 226–243 (2008).
2. Herman, A., Kappler, J. W., Marrack, P. & Pullen, A. M. Superantigens: mechanism of T-cell stimulation and role in immune responses. *Annu Rev. Immunol.* **9**, 745–772 (1991).
3. Levy, R. et al. Superantigens hyperinduce inflammatory cytokines by enhancing the B7-2/CD28 costimulatory receptor interaction. *Proc. Natl. Acad. Sci. USA* **113**, E6437–E6446 (2016).

4. Dellabona, P. et al. Superantigens interact with MHC class II molecules outside of the antigen groove. *Cell* **62**, 1115–1121 (1990).
5. Seth, A. et al. Binary and ternary complexes between T-cell receptor, class II MHC and superantigen in vitro. *Nature* **369**, 324–327 (1994).
6. Givan, A. L., Fisher, J. L., Waugh, M., Ernstoff, M. S. & Wallace, P. K. A flow cytometric method to estimate the precursor frequencies of cells proliferating in response to specific antigens. *J. Immunol. Methods* **230**, 99–112 (1999).
7. Marrack, P. & Kappler, J. The staphylococcal enterotoxins and their relatives. *Science* **248**, 1066 (1990).
8. McCormick, J. K., Yarwood, J. M. & Schlievert, P. M. Toxic shock syndrome and bacterial superantigens: An update. *Annu Rev. Microbiol* **55**, 77–104 (2001).
9. Miethke, T. et al. T cell-mediated lethal shock triggered in mice by the superantigen staphylococcal enterotoxin B: Critical role of tumor necrosis factor. *J. Exp. Med* **175**, 91–98 (1992).
10. Chua, K. Y. et al. The dominant Australian community-acquired methicillin-resistant Staphylococcus aureus clone ST93-IV [2B] is highly virulent and genetically distinct. *PloS one* **6**, e25887 (2011).
11. Chen, Z. et al. Humanized transgenic mice expressing HLA DR4-DQ3 haplotype: reconstitution of phenotype and HLA-restricted T-cell responses. *Tissue Antigens* **68**, 210–219 (2006).
12. Xu, S. X., Kasper, K. J., Zeppa, J. J. & McCormick, J. K. Superantigens modulate bacterial density during staphylococcus aureus nasal colonization. *Toxins (Basel)* **7**, 1821–1836 (2015).
13. Xu, S. X. et al. Superantigens subvert the neutrophil response to promote abscess formation and enhance Staphylococcus aureus survival in vivo. *Infect. Immun.* **82**, 3588–3598 (2014).
14. Islander, U. et al. Superantigenic Staphylococcus aureus stimulates production of interleukin-17 from memory but not naive T cells. *Infect. Immun.* **78**, 381–386 (2010).
15. Yomogida, K., Chou, Y. K. & Chu, C. Q. Superantigens induce IL-17 production from polarized Th1 clones. *Cytokine* **63**, 6–9 (2013).
16. Szabo, P. A. et al. Rapid and rigorous IL-17A production by a distinct subpopulation of effector memory T lymphocytes constitutes a novel mechanism of toxic shock syndrome immunopathology. *J. Immunol.* **198**, 2805–2818 (2017).
17. Zheng, M. Z. M. et al. Single-cycle influenza virus vaccine generates lung CD8(+) Trm that cross-react against viral variants and subvert virus escape mutants. *Sci. Adv.* **9**, eadg3469 (2023).
18. Zhao, Y. et al. Toxins targeting the Kv1.3 Channel: Potential immunomodulators for autoimmune diseases. *Toxins (Basel)* **7**, 1749–1764 (2015).
19. Canas, C. A., Castano-Valencia, S. & Castro-Herrera, F. Pharmacological blockade of KV1.3 channel as a promising treatment in autoimmune diseases. *J. Transl. Autoimmun.* **5**, 100146 (2022).
20. Beeton, C. et al. Targeting effector memory T cells with a selective peptide inhibitor of Kv1.3 channels for therapy of autoimmune diseases. *Mol. Pharm.* **67**, 1369–1381 (2005).
21. Chiang, E. Y. et al. Potassium channels Kv1.3 and KCa3.1 cooperatively and compensatorily regulate antigen-specific memory T cell functions. *Nat. Commun.* **8**, 14644 (2017).
22. Matheu, M. P. et al. Imaging of effector memory T cells during a delayed-type hypersensitivity reaction and suppression by Kv1.3 channel block. *Immunity* **29**, 602–614 (2008).
23. Holz, L. E. et al. CD8(+) T cell activation leads to constitutive formation of liver tissue-resident memory T cells that seed a large and flexible niche in the liver. *Cell Rep.* **25**, 68–79.e64 (2018).
24. Zheng, M. Z. M. & Wakim, L. M. Tissue resident memory T cells in the respiratory tract. *Mucosal Immunol.* **15**, 379–388 (2022).
25. Braverman, J. et al. Staphylococcus aureus specific lung resident memory CD4(+) Th1 cells attenuate the severity of influenza virus induced secondary bacterial pneumonia. *Mucosal Immunol.* **15**, 783–796 (2022).
26. Lin, Y. S. et al. In vivo induction of apoptosis in immature thymocytes by staphylococcal enterotoxin B. *J. Immunol.* **149**, 1156–1163 (1992).
27. Mahlknecht, U., Herter, M., Hoffmann, M. K., Niethammer, D. & Dannecker, G. E. The toxic shock syndrome toxin-1 induces anergy in human T cells in vivo. *Hum. Immunol.* **45**, 42–45 (1996).
28. Watson, A. R., Janik, D. K. & Lee, W. T. Superantigen-induced CD4 memory T cell anergy. I. Staphylococcal enterotoxin B induces Fyn-mediated negative signaling. *Cell Immunol.* **276**, 16–25 (2012).
29. Janik, D. K. & Lee, W. T. Staphylococcal Enterotoxin B (SEB) Induces Memory CD4 T Cell Anergy in vivo and Impairs Recall Immunity to Unrelated Antigens. *J. Clin. Cell Immunol.* **6**, 1–8 (2015).
30. Arvand, M. & Hahn, H. T-cell activation and proliferation in a case of recurrent menstrual toxic shock syndrome. *Zentralbl Bakteriol.* **284**, 164–169 (1996).
31. Meilleur, C. E. et al. Bacterial superantigens expand and activate, rather than delete or incapacitate, preexisting antigen-specific memory CD8+ T cells. *J. Infect. Dis.* **219**, 1307–1317 (2019).
32. Rasigade, J. P. et al. T-cell response to superantigen restimulation during menstrual toxic shock syndrome. *FEMS Immunol. Med Microbiol* **62**, 368–371 (2011).
33. Cauley, L. S., Cauley, K. A., Shub, F., Huston, G. & Swain, S. L. Transferable anergy: superantigen treatment induces CD4+ T cell tolerance that is reversible and requires CD4-CD8- cells and interferon gamma. *J. Exp. Med* **186**, 71–81 (1997).
34. Tuffs, S.- W., Haeryfar, S.- M.- M. & McCormick, J.- K. Manipulation of innate and adaptive immunity by staphylococcal superantigens. *Pathogens* **7**, 53 (2018).
35. Kolata, J. B. et al. The fall of a dogma? unexpected high T-cell memory response to staphylococcus aureus in humans. *J. Infect. Dis.* **212**, 830–838 (2015).
36. Hendriks, A. et al. Staphylococcus aureus-specific tissue-resident memory CD4(+) T cells are abundant in healthy human skin. *Front Immunol.* **12**, 642711 (2021).
37. Holtfreter, S. et al. egc-Encoded superantigens from Staphylococcus aureus are neutralized by human sera much less efficiently than are classical staphylococcal enterotoxins or toxic shock syndrome toxin. *Infect. Immun.* **72**, 4061–4071 (2004).
38. Park, J. Y., Kim, J. S. & Woo, H. Prevalence of antibody to toxic shock syndrome toxin-1 in burn patients. *Ann. Lab. Med.* **35**, 89–93 (2015).
39. Parsonnet, J. et al. Prevalence of toxic shock syndrome toxin 1 (TSST-1)-producing strains of Staphylococcus aureus and antibody to TSST-1 among healthy Japanese women. *J. Clin. Microbiol* **46**, 2731–2738 (2008).
40. Tuffs, S.W. et al. Superantigens promote Staphylococcus aureus bloodstream infection by eliciting pathogenic interferon-gamma production. *Proc. Natl. Acad. Sci. USA* **119**, e2115987119 (2022).
41. Nguyen, T. H. et al. Influenza, but not SARS-CoV-2, infection induces a rapid interferon response that wanes with age and diminished tissue-resident memory CD8(+) T cells. *Clin. Transl. Immunol.* **10**, e1242 (2021).
42. Pizzolla, A. et al. Influenza-specific lung-resident memory T cells are proliferative and polyfunctional and maintain diverse TCR profiles. *J. Clin. Invest* **128**, 721–733 (2018).
43. Bedoui, S. et al. Cross-presentation of viral and self antigens by skin-derived CD103+ dendritic cells. *Nat. Immunol.* **10**, 488–495 (2009).
44. Oxenius, A., Bachmann, M. F., Zinkernagel, R. M. & Hengartner, H. Virus-specific MHC-class II-restricted TCR-transgenic mice: effects on humoral and cellular immune responses after viral infection. *Eur. J. Immunol.* **28**, 390–400 (1998).
45. Townsend, A. R. et al. The epitopes of influenza nucleoprotein recognized by cytotoxic T lymphocytes can be defined with short synthetic peptides. *Cell* **44**, 959–968 (1986).

46. Mamalaki, C. et al. Positive and negative selection in transgenic mice expressing a T-cell receptor specific for influenza nucleoprotein and endogenous superantigen. *Dev. Immunol.* **3**, 159–174 (1993).
47. Ge, C. et al. Neutrophils play an ongoing role in preventing bacterial pneumonia by blocking the dissemination of Staphylococcus aureus from the upper to the lower airways. *Immunol. Cell Biol.* **98**, 577–594 (2020).
48. Monk, I. R. & Stinear, T. P. From cloning to mutant in 5 days: Rapid allelic exchange in Staphylococcus aureus. *Access Microbiol* **3**, 000193 (2021).
49. Gill, S. R. et al. Insights on evolution of virulence and resistance from the complete genome analysis of an early methicillin-resistant Staphylococcus aureus strain and a biofilm-producing methicillin-resistant Staphylococcus epidermidis strain. *J. Bacteriol.* **187**, 2426–2438 (2005).
50. Monk, I. R., Tree, J. J., Howden, B. P., Stinear, T. P. & Foster, T. J. Complete bypass of restriction systems for major staphylococcus aureus lineages. *mBio* **6**, e00308–e00315 (2015).
51. Bedford, J. G. et al. Unresponsiveness to inhaled antigen is governed by conventional dendritic cells and overridden during infection by monocytes. *Sci. Immunol* **5**, eabb5439 (2020).
52. Wakim, L. M., Woodward-Davis, A. & Bevan, M. J. Memory T cells persisting within the brain after local infection show functional adaptations to their tissue of residence. *Proc. Natl. Acad. Sci. USA* **107**, 17872–17879 (2010).

Acknowledgements

This work was supported by the National Health and Medical Research Council of Australia (LMW, TPS) and the Australian Research Council (TPS, IM). Figures 5a, i - created in BioRender. Wakim, L. (2024) BioRender.com/w79t204.

Author contributions

I.M. and L.M.W. conceived the study. H.Z., L.M.W., J.B., I.M. performed experimental studies and analyzed the data. C.J. and A.B. provided key reagents L.M.W., and T.S., supervised the work.

Competing interests

The authors declare no competing interests.

Additional information

Supplementary information The online version contains supplementary material available at https://doi.org/10.1038/s41467-024-54074-8.

Correspondence and requests for materials should be addressed to Linda M. Wakim.

Peer review information *Nature Communications* thanks Jon Houtman, Andrew Snow and the other, anonymous, reviewer(s) for their contribution to the peer review of this work. A peer review file is available.